CurvedTouch: Effects of Surface Curvature and Cursor Mapping Method for XR Touch Input on Curved Surface

YUBIN LEE*, KAIST, Republic of Korea
LIWEI CHAN, National Yang Ming Chiao Tung University, Taiwan
GEEHYUK LEE, KAIST, Republic of Korea
SANG HO YOON, KAIST, Republic of Korea

Extended reality (XR) systems now use everyday physical surfaces as touch input spaces. However, existing systems rely primarily on flat surfaces due to the given device form factor and sensing capabilities. Despite advancements in sensing technologies that allow touch input across surfaces with diverse curvatures, the effects of surface curvature on user behavior and performance in indirect XR touch interaction remain underexplored. To this end, we present CurvedTouch, a study that investigates the effects of surface curvature and cursor mapping methods on XR indirect touch interaction. We evaluated 4 surface curvatures (flat, R = 75mm, 60mm, and 45mm) and two cursor mapping methods (Projection-based and Distance-based) in a within-subject study by measuring task performance, behavioral pattern, workload, and usability. 16 participants performed the indirect Tap, Drag, and Trace task under certain conditions. Our results reveal that the task performance and usability significantly dropped for a curvature between R = 45mm and R = 60mm. As curvature increases, users change their input strategy from finger-level motion to whole-hand movement. Unlike prior findings in direct touch interaction, we found that minimum button size increases on a high curvature surface in an indirect touch scenario. For the cursor mapping method, distance-based mapping showed higher usability under high curvature. Based on these findings, we came up with design guidelines for interaction type, button size, interaction area, and cursor mapping method for the XR indirect touch interface on a curved surface.

CCS Concepts: • **Human-centered computing → Interaction design process and methods**; **Systems and tools for interaction design**; **Interactive systems and tools**.

Additional Key Words and Phrases: Extended Reality, Touch Input, Curved Surface, User Behavior, Interface Design, Design Guideline

ACM Reference Format:
Yubin Lee, Liwei Chan, Geehyuk Lee, and Sang Ho Yoon. 2026. CurvedTouch: Effects of Surface Curvature and Cursor Mapping Method for XR Touch Input on Curved Surface. *Proc. ACM Interact. Mob. Wearable Ubiquitous Technol.* 10, 2, Article 52 (June 2026), 29 pages. https://doi.org/10.1145/3810236

1 INTRODUCTION

Recent research on XR input increasingly focuses on utilizing everyday surfaces as touchable interfaces. Utilizing everyday surfaces as touch interfaces addressed issues such as the lack of tactile feedback and fatigue associated with mid-air gestures [18]. It is also advantageous to use everyday surfaces for mobile environments, since no separate controller is required. Moving beyond traditional approaches that detect touch events from the perspective of the touched surface, researchers have explored techniques that infer touch based on the touching

*corresponding author

Authors' Contact Information: Yubin Lee (corresponding author), KAIST, Daejeon, Republic of Korea, dkch3236@kaist.ac.kr; Liwei Chan, Hsinchu, National Yang Ming Chiao Tung University, Taiwan, liweichan@nycu.edu.tw; Geehyuk Lee, KAIST, Daejeon, Republic of Korea, geehyuk@kaist.ac.kr; Sang Ho Yoon, KAIST, Daejeon, Republic of Korea, sangho@kaist.ac.kr.

ACM 2474-9567/2026/6-ART52
https://doi.org/10.1145/3810236

hand itself, using finger color changes or motion dynamics [24, 33, 50]. These approaches enable the detection of touch timing, location, and even touch intensity without requiring sensors embedded in the surface. Building on this technological foundation, several studies implement and evaluate XR interaction systems that utilize everyday surfaces in the user's environment, such as walls, desks, and furniture, as touch interfaces [6, 37].

Unlike conventional touch screens, everyday touchable surfaces are not flat but consist of various curvatures. Still, no in-depth research has explored how the geometry of touch surfaces in XR environments influences the user's input behavior and performance.

Surface geometry fundamentally influences how users touch and interact with the surface [20]. As surface geometry changes, users may adopt different finger postures, movement strategies, or levels of precision when performing touch input. These behavioral differences suggest that interface design parameters (Types of interactions or the layout of interface elements) should be adapted according to surface curvature. However, there is still a limited understanding of how interaction strategies and design-relevant user behaviors vary across different curved surfaces in XR contexts.

Touch interaction is generally divided into two categories, direct touch and indirect touch. Direct touch describes a situation where the location the user touches and the location of the interface being manipulated are identical. The user can see both their hand and the interface simultaneously during interaction. Curved displays and OmniTouch [13] are examples of direct touch interfaces. On the other hand, indirect touch refers to situations in which the user's touch location and the manipulated interface are spatially separated, as is common in XR user interfaces. Users perform the touch interaction while seeing only one of their hands or only the given visual interface. Examples of indirect touch scenarios include a laptop trackpad, Tripad's indirect input mode [6], or T2IRay [22].

Our work focuses mainly on indirect touch. Since existing research on touch input on curved surfaces has been limited to direct touch scenarios, we shift our focus to upcoming XR environments where virtual or augmented content often does not align with touching surfaces [12].

Unlike direct touch on curved surfaces, indirect touch introduces an additional challenge. Since the hand and cursor are positioned at different locations during indirect touch, the mapping of the actual finger movement to the cursor movement becomes a critical issue. This issue becomes more apparent on curved surfaces, where surface curvature creates a mismatch between the finger's three-dimensional (3D) movement and the cursor's two-dimensional (2D) motion. Therefore, existing interaction designs based on direct or flat-surface touch are difficult to apply directly to indirect touch scenarios on curved surfaces.

To address this research gap, we investigate how the curvature of touch surfaces in XR environments affects users' performance, usability, and behavioral patterns through both quantitative and qualitative analyses. We also examine how different strategies for mapping touch input on curved surfaces to planar cursor movement influence user experience and performance. Based on our findings, we derive practical design guidelines for creating XR touch interfaces on curved surfaces (Fig. 1). We aim to extend the physical touch input space in XR beyond flat surfaces such as walls and desks toward truly arbitrary everyday surfaces. We address the following research questions:

- **RQ1.** How does surface curvature affect users' task performance and usability in indirect touch interaction on curved-surfaces?
- **RQ2.** How does surface curvature influence users' behavioral patterns during indirect touch interaction on curved-surfaces?
- **RQ3.** How should the 3D movement of a fingertip on a curved surface be mapped to a 2D cursor position to assist user performance and usability?

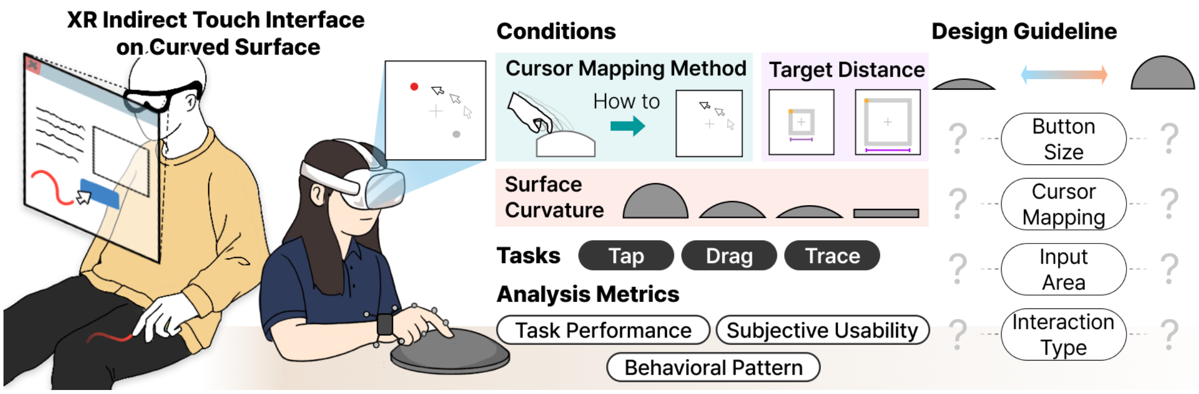

Fig. 1. Overview of CurvedTouch. We designed a within-subjects study to collect XR indirect touch input data under 4 surface curvatures, 2 cursor mapping methods, and 2 target distance conditions. We analyzed task performance, usability, and behavioral patterns, leading to proposed design guidelines for XR touch interfaces on curved surfaces.

2 RELATED WORK

2.1 Touch Interaction on Physical Surface in XR

Touch interaction on physical surfaces offers several advantages in XR environments. By involving physical contact, surface-based interaction naturally provides tactile feedback, which improves input precision and user confidence [4, 29]. In addition, since users do not need to keep their hands suspended in mid-air, surface-based interaction can also reduce physical fatigue, making it suitable for prolonged use in XR scenarios. Early related studies used touch-enabled devices such as smartphones or tablets held by the user [28, 39, 41], or attached touch sensors to specific physical surfaces such as the HMD housing [8].

Subsequent work extended this idea beyond predefined devices or surfaces and investigated touch recognition on arbitrary physical surfaces. This was a transition from instrumenting "the surface being touched" to sensing "the fingers performing the touch". Researchers have utilized HMD hand-tracking data or additional vision data to detect touch actions [10, 11, 13, 17, 24, 32, 50]. Some systems combine acoustic sensors to capture vibrations or sounds generated by finger tapping to compensate for vision-based approaches [21, 30, 34, 51].

Given the ability to recognize finger touch on arbitrary physical surfaces, several studies have attempted to implement classic input interfaces such as track pads [6] and QWERTY keyboards [9, 36, 37, 40, 53] in XR environments. However, most studies constrain the geometry of the input surface to a flat plane. Although recent work [9] includes experiments and analysis on typing on curved objects such as cups and water bottles, this work only concludes that users are less familiar with curved surfaces than flat ones, leading to lower typing speed and accuracy. Thus, a systematic analysis of touch input grounded in surface curvature is timely, given the growing adoption of XR systems capable of utilizing everyday surfaces for touch input.

2.2 On-body Touch Interfaces

Although XR touch interfaces using physical surfaces have mostly been designed for planar surfaces, there is a line of research on XR touch interfaces for non-planar surfaces. Those works primarily focused on "on-body interaction", where the user's body functions as the input surface [3, 14, 16, 52]. The user's body served as a promising input surface for XR environments and wearable devices. On-body interaction offers the advantage of being readily available without external devices or environmental dependencies, and it enables input grounded in the user's proprioceptive and tactile senses [3, 14, 52]. Furthermore, on-body interaction causes less physical fatigue and is more socially acceptable than freehand interaction [16].

Prior research has proposed on-skin touch recognition systems [33, 47] and interfaces that utilize various body parts, such as the arm [42, 54], thigh [31, 43], palm [5, 19, 23, 25, 35, 45, 46] as input spaces. These studies have primarily examined factors such as the spatial characteristics of body parts, accessibility, memorability, and usability under different postures. However, prior on-body interaction research has paid limited attention to how the geometric properties of the surface itself influence users' behavioral patterns on touch input. Therefore, this suggests that the effect of surface curvature on the behavioral pattern has not been fully examined and needs further exploration.

2.3 Touch Input on Non-planar Surfaces

Outside the XR context, existing HCI research has conducted various studies to understand the characteristics of touch input on non-planar surfaces, especially on non-planar displays. Previous work concludes that curved and 3D displays with depth-aware interaction represent an important research direction that complements flat interfaces, suggesting a need for new interface designs leveraging the unique characteristics of new form factor [2].

In response, Roudaut et al. [38] demonstrated through a target selection task on a hemispherical surface that surface curvature and convexity/concavity directly affect touch offset and accuracy. Based on this, they proposed guidelines for button size in curved interface design. Subsequent studies revealed that input accuracy on deformable hemispherical touch surfaces heavily depends on visual feedback and surface shape, highlighting the need for designs that consider geometric characteristics of curved surfaces [1]. In large interactive environments, research on user input performance on curved surfaces has centered around displays that connect horizontal and vertical planes via curved surfaces. BendDesk [48] analyzed dragging and pointing performance in a desk environment with curved connections between horizontal and vertical planes, demonstrating that touch inputs across curved surfaces are slower and less stable than flat surfaces, imposing additional fatigue on users.

Extending these findings, Voelker et al. [44] experimentally analyzed flicking gesture accuracy in a similar environment. They found that flicking accuracy varies depending on surface continuity, input location, and body alignment, with errors in the motor execution phase having a greater impact than visual perception errors. A recent study analyzed the effects of hinge curvature radius for foldable displays. Zinck et al.'s research quantitatively demonstrated that smaller hinge curvature improves drag performance and user preference, highlighting the critical role of geometric characteristics at curved junctions in input performance [55].

To summarize, previous studies have emphasized that touch surfaces on curved surfaces should be studied separately from those on flat surfaces because the shape of the touch surface significantly impacts input performance and usability. However, these prior studies primarily examined direct touch on curved surfaces, where the visual interface and the touched physical surface are spatially coupled. In contrast, we focus on indirect touch in XR, where the touched curved surface and the manipulated visual interface are spatially separated. This distinction is important because indirect touch introduces an additional mapping problem between fingertip movement on a 3D curved surface and cursor motion on a 2D interface plane, which may lead to behavioral and usability patterns that differ from those reported in prior direct-touch studies.

3 METHODOLOGY

3.1 Surface Curvature Conditions

Given that on-body interaction represents one of the most actively explored approaches in research on non-planar surface interaction in XR environments, we designed the experimental conditions based on the curvature of body parts commonly used as input spaces, namely the arm and the leg. Accordingly, we adopted body-based surfaces as references for touch interfaces in XR and included four surface curvature conditions, consisting of three curved surfaces and a flat surface (R=∞) as a baseline.

Each curvature radius was derived based on anthropometric data. Specifically, each body part was approximated as a perfect cylinder, so the curvature radius was obtained by dividing the average circumference by 2π. However, this circular approximation yields a surface that is more curved than the actual body surface typically contacted during on-body interaction, as real body parts are generally flatter than a perfect circle. As a result, the diameter derived from circumference alone would overestimate surface curvature. To compensate for this, we applied a shape correction by scaling the diameter using the ratio between the average circumference and the average width, normalized by π. This normalization ensures that the scaling factor equals 1 for a perfectly circular cross-section, while increasing the diameter for flatter shapes. Finally, for practical reasons related to analysis and surface fabrication, the resulting curvature radii were rounded to the nearest 5mm increment.

Based on this process, the curvature radii were set to 75mm for the thigh, 60mm for the upper arm, and 45mm for the forearm and wrist. Although the palm is frequently used as an input space in on-body interaction, it was excluded from the curvature definition because its surface is relatively close to planar. Concave surfaces were also excluded, as they are uncommon in everyday interaction contexts.

These body-part measurements were used only as references for selecting representative curvature magnitudes. The experimental surfaces themselves were not intended to faithfully reproduce the geometry of specific body parts. Thus, we adopted hemispherical surfaces rather than cylindrical surfaces because they provide uniform curvature across all movement directions, allowing surface curvature to be isolated as a controlled variable.

3.2 Curved Surface Fabrication and Touch Sensing

As reviewed in the Related Work section, a variety of sensing techniques have been proposed to detect touch on arbitrary surfaces. However, the goal of this study is not to introduce a new technique for sensing touch on curved surfaces, but rather to analyze touch input in scenarios where curved surface touch interaction is already supported. Therefore, among the possible implementation options, we chose capacitive sensing because it enabled real-time and robust touch event detection on all fabricated surfaces without requiring model training or wearing additional hand-held equipment. This choice allowed us to focus on the design and evaluation of touch interaction on curved surfaces, rather than on the performance of the touch-sensing technique itself.

The input surfaces used in the experiment were fabricated according to the four predefined curvature conditions. Each curved surface was modeled as a segment of a sphere with the specified curvature radius, cut such that the base diameter was 90mm. For the flat condition, a 90mm diameter circular disk was used. All surfaces were fabricated using a 3D printer, then sanded and coated with conductive paint. The coated surfaces were connected to an Arduino to detect finger contact.

To capture the precise location of the touch on the surface, we attached markers to the participant's finger and tracked them using an OptiTrack motion capture system. This allowed us to record the finger position at the moment of touch with high spatial accuracy. The location of the touch was estimated from the position of the marker attached to the participant's index fingernail at the time the touch was detected.

3.3 Cursor Mapping Method

For discrete interactions such as Tap, the hand moves through the air and makes brief, momentary contact with the surface. The input is therefore defined by a single contact location at lift-off, and the finger's continuous trajectory does not contribute to the command. As a result, mapping 3D finger motion on a curved surface to 2D cursor movement is not a concern for Tap.

In contrast, continuous interactions such as Drag require the finger to move while maintaining contact with the surface. Here, the input is defined by the finger's continuous 3D path along the curved surface, which must

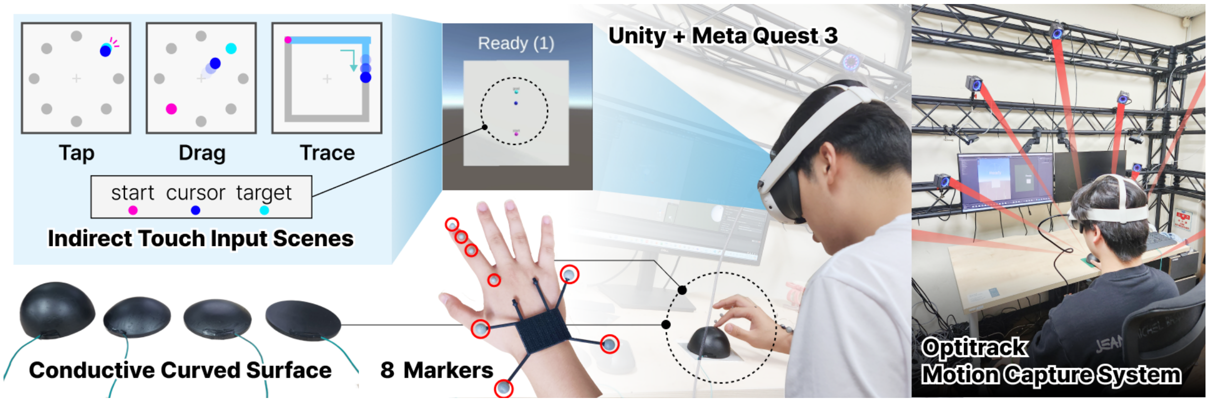

Fig. 2. The experimental setup. We implemented three types of touch interaction tasks, including Tap, Drag, and Trace, in Unity with Meta Quest 3. We attached a total of 8 markers to the user's hand: 4 markers on the index finger tip and each joint (DIP, PIP, MCP), and 4 markers on the wrist to form a rigid body. An OptiTrack system with 12 motion capture cameras tracked the markers, storing the user's hand posture data and recognizing the touch position. For the touchable surfaces with four different curvatures, conductive paint was applied and connected to a microcontroller to sense touch. During the experiment, all surfaces were fixed in one position using a mount attached to the desk.

be converted into cursor motion on a 2D screen plane. This makes the cursor-mapping method a key design choice, motivating our investigation of how different mappings affect performance and experience.

This study first defines a baseline approach for mapping finger motion on curved surfaces to 2D cursor movement in indirect, continuous-touch interaction, and then systematically evaluates how alternative mappings affect touch input. A continuous touch action can be characterized by its start point, movement trajectory, and end point. Because the start point coincides with the current cursor position, we distinguish two mapping strategies based on what primarily drives cursor movement: the fingertip's terminal position or its motion trajectory.

- **Projection-based Method (PM).** In this method, the cursor position is determined by projecting the finger's movement onto the base plane of the curved surface. This approach assumes that users estimate cursor position mainly from the finger's final position, thereby maintaining continuity with familiar 2D touch interaction.
- **Distance-based Method (DM).** In this method, cursor movement direction is defined using the same projection, while movement distance is determined by the actual 3D path length traveled along the curved surface. This strategy reflects an interaction model in which users rely more directly on the physical movement trajectory, aligning cursor control with proprioceptive feedback.

4 USER STUDY: XR TOUCH INPUT MOTION DATA COLLECTION ON CURVED SURFACES

We conducted a user study to investigate how indirect touch interaction in XR on curved surfaces is influenced by surface curvature and cursor mapping strategies. In particular, we examined how variations in surface curvature affect users' task performance, perceived usability, and behavioral patterns, as well as how different cursor mapping methods interact with surface curvature.

Participants performed a set of representative touch interaction tasks under four surface curvature conditions and two cursor mapping methods. In addition to task performance and subjective evaluations, we collected data on finger joint rotation, wrist movement, and clutching behavior to capture changes in users' input behavior. Through this study, we aim to understand not only whether performance differs across curved surfaces but

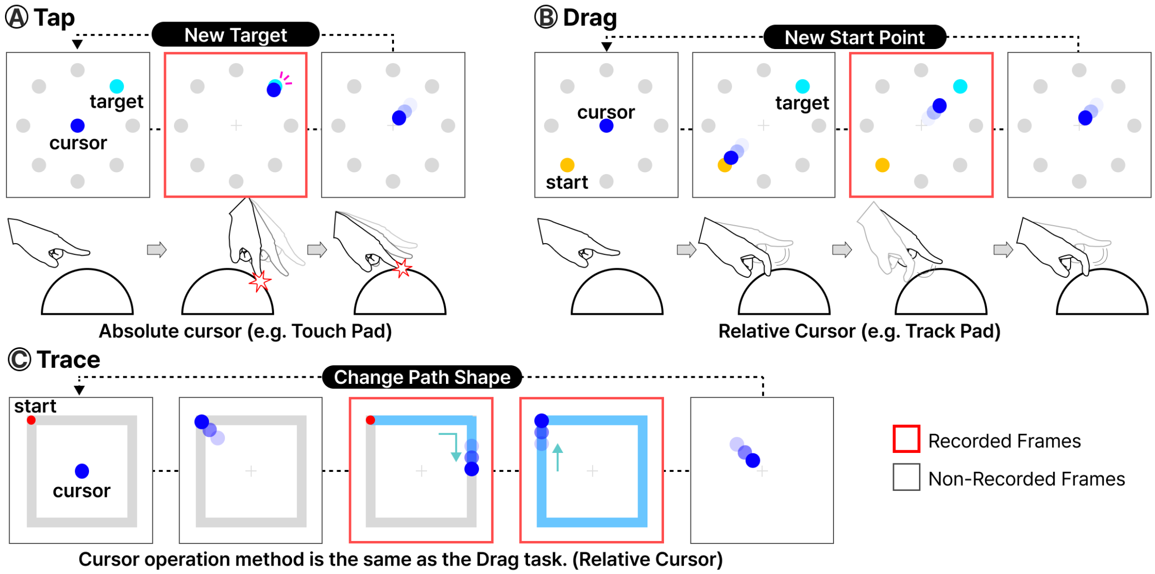

Fig. 3. We used three distinct tasks: (a) Tap, (b) Drag, and (c) Trace. The Tap task employed an absolute cursor that moved in real-time with the fingertip, even during hovering. For the other tasks, a relative cursor was used, which moved only when the hand was in contact with the surface and remained stationary when lifted. Frames during task execution where the data were recorded were marked with a red border. In all tasks, users were instructed to move the cursor back to the origin at the end of each trial.

also how users adapt their touch strategies in response to surface geometry and how such adaptations relate to performance and usability outcomes.

4.1 Study Setup

We recruited 16 adult participants (8 female) for the study. Two participants were left-handed, but both reported routinely using everyday touch interfaces with their right hand. Participants received monetary compensation upon completion of the experiment.

Fig. 2 shows the configuration of the experimental apparatus. The experiment was conducted in a VR environment. The system consisted of a Meta Quest 3 head-mounted display and an OptiTrack motion capture system. To precisely track index finger motion, we attached markers to the fingertip and each joint of the participant's index finger (MCP, PIP, DIP). A rigid body composed of four markers was attached to the wrist to capture wrist movement.

The experimental interaction scene was implemented in Unity. During the experiment, participants interacted with an on-screen cursor presented on a virtual 2D screen in VR. We provided the cursor as a visual proxy for the estimated touch location on the surface. No other visual aids were provided, such as a virtual hand model or a visual rendering of the physical touch surface.

4.2 Tasks

In this experiment, participants performed three tasks in VR: Tap representing discrete input, and Drag and Trace representing continuous input (Fig.3).

Tap. (Fig.3-A) Participants selected targets on a virtual screen floating in front of them in VR by controlling an on-screen cursor. The cursor was rendered as a point projected onto a plane parallel to the base of the curved surface, and it remained visible regardless of whether the participant's finger was in contact with the physical surface. A tap was registered as a touch followed by a lift-off; at the moment of lift-off, the system logged both the fingertip position and the corresponding cursor position. When the cursor successfully tapped the target, the target disappeared, and the participant was prompted to return the cursor to the origin by tapping the center crosshair on the virtual screen. Once this center tap was completed, the next target appeared. Targets were presented one at a time at one of eight locations equally spaced in direction and equal in distance from the origin.

Drag. (Fig.3-B) Participants dragged the on-screen cursor from a start point to a target point on the virtual screen. The cursor behaved like a standard mouse cursor: it moved only while the hand was in contact with the surface and remained stationary when the hand was lifted. During contact, cursor motion followed the cursor-mapping method assigned to the current condition (as described in the previous section). Each trial began with only the start point visible. The participant first moved the cursor to this start point, which appeared at one of eight locations equidistant from the screen center (matching the Tap task layout). Once the cursor reached the start point, the target point appeared at the diametrically opposite location relative to the origin. At that moment, we began recording the hand-marker positions, cursor position, and surface contact state. Recording continued until the participant dragged the cursor into the target. After a successful hit, the start and target points disappeared and a center crosshair appeared. The participant then returned the cursor to the screen center; upon reaching it, the next start point appeared, initiating the next trial.

Trace. (Fig.3-C) Participants traced a closed path on the virtual screen, starting from a designated start point, moving clockwise, and returning to the start point to complete the trial. Cursor motion and contact behavior followed the same rules as in the Drag task. Each trial began by displaying a path and its start point. Participants first moved the cursor onto the start point; once reached, the system prompted them to begin tracing. Recording of hand-marker position, cursor position, and surface contact status started when the cursor first left the start point (i.e., at trace onset). To avoid mistakenly treating this initial departure as an immediate "return" to the start point, the trial ended only after (1) a minimum time had elapsed and (2) the cursor subsequently reached the start point again. After completion, the system prompted participants to move the cursor back to the origin. When the cursor reached the origin, the next path and its start point appeared, and the participant again moved to the start point to begin the next trial. We used circles and squares as path shapes presented in strict alternation (no consecutive repeats). The start point was the top-left corner for squares and the highest point for circles. Users were instructed to always trace clockwise, regardless of the path type.

4.3 Experiment Design

For Tap task, we conducted a 4×2 within-subject study with 2 variables; *Surface Curvature* and *Target Distance*. For Drag and Trace task, we conducted 4×2×2 within-subject study with 3 variables; *Surface Curvature*, *Cursor Mapping Method* and *Target Distance*. The conditions for each independent variable are described below (Fig. 4).

- **Surface Curvature** (Fig.4-A) 4 curvature conditions were tested: a flat surface ($R = \infty$) and three convex spherical surfaces with curvature of $R = 75$mm, $R = 60$mm, and $R = 45$mm.
- **Cursor Mapping Method** (Fig. 4-B) 2 cursor mapping strategies were evaluated: the Projection-based method and the Distance-based method.
- **Target Distance** (Fig. 4-C) To examine the influence of interface scale, 2 target distances (3 cm and 6 cm) were selected based on the functional range of index finger movement.

Accordingly, a total of 8 experimental conditions were created for the Tap task, and 16 conditions for the Drag and Trace tasks. To mitigate order effects, a Latin Square design was used to arrange the conditions in a balanced sequence.

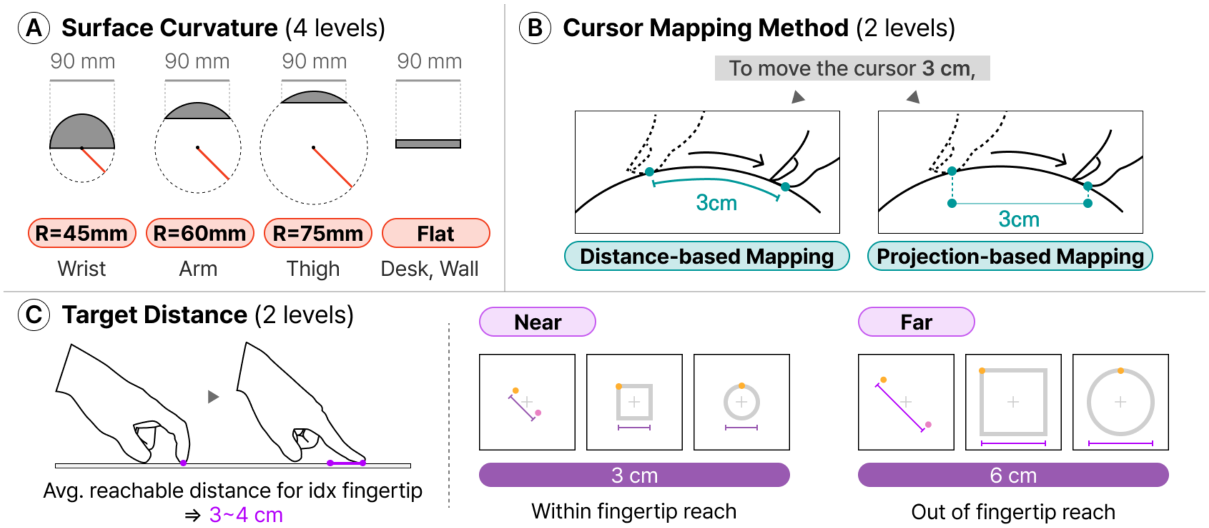

Fig. 4. Conditions used in the experiment. (a) *Surface Curvature*. 4 curvature levels were used: the baseline flat condition plus curvature conditions derived from 3 commonly used everyday curved surfaces. (b) *Cursor Mapping Method*. Two cursor mapping methods were proposed. Distance-based Mapping (DM) moves the cursor by the cumulative 3D distance traveled by the fingertip. Projection-based Mapping (PM) moves the cursor based on the change in the projected fingertip position on the base. (c) *Target Distance*. Considering that the average distance the index finger tip can move when touching a surface is 3 4 cm, we experimented with two types of interactions: Near (3 cm) and Far (6 cm).

The experiment was organized into sessions. In each session, participants completed the Tap, Drag, and Trace tasks in that fixed order. Each participant completed 16 sessions in total. Within a session, Surface Curvature and Target Distance were held constant, and the Cursor Mapping Method was fixed for the tasks that used it (Drag and Trace; this factor did not apply to Tap). Accordingly, Drag and Trace had one session per condition, whereas Tap had two sessions per condition. Each session included 24 Tap trials, 24 Drag trials, and 10 Trace trials. For Tap and Drag, trials were arranged as three 8-trial blocks: in each block, all eight target directions appeared exactly once, in randomized order. Repeating the block three times yielded 24 trials (8 directions × 3 repetitions). For Trace, participants traced two path shapes, square and circle, which alternated and were repeated five times, yielding 10 trials (2 paths × 5 repetitions).

4.4 Procedure

Before the experiment, participants received an overview of the required equipment, collected data, tasks, duration, and compensation, and then signed the consent form. They next completed a short training session under the same settings as their first experimental session to familiarize themselves with the input system. Participants then performed 16 sessions in the Latin-square order. During a session, they could request an undo if a trial was incorrectly recorded due to an input error. After each session, participants removed the HMD and completed a brief questionnaire assessing that condition (Workload, Ease of Use, and Satisfaction). Breaks were allowed at any time between sessions.

Table 1. Measurement Metrics used in the Study.

Metric (Task)	**Unit**	**Description**
Task Performance		
Offset (Tap) [38]	mm	Mean distance between touch points and target centers
Spread (Tap) [38]	mm	Required button size to cover 95% of touch points
Throughput (Drag) [26]	bps	Speed-accuracy efficiency during target acquisition
Movement Error (Trace) [27]	mm	Average deviation from the intended tracing path
Movement Variability (Trace) [27]	mm	Consistency of tracing accuracy across the path
Behavioral Pattern (Drag, Trace)		
Joint Angle Range	degrees	Range of index finger joint angles (MCP, PIP, DIP)
Wrist Movement Distance	m	Total 3D movement distance of the wrist during each trial
Clutching Count	–	Number of finger lift-and-recontact actions during a task
Clutching Distance	m	Mean finger movement distance before a clutch occurs
Subjective Evaluation		
Raw NASA-TLX [15]	–	Perceived workload across 6 cognitive and physical dimensions
Ease of Use, Satisfaction	–	User's subjective ratings on comfort and preference

4.5 Evaluation Metrics

User interaction was evaluated using task performance metrics, behavioral pattern metrics, and subjective evaluations. Table 1 summarizes all metrics used in the study.

4.5.1 Task Performance Metrics.

- **Tap Task.** *Offset* [38] The Euclidean distance between each touch point and its corresponding target center.

$$\text{Offset} = \frac{1}{N}\sum_{i=1}^{N} \|\mathbf{p}_i - \mathbf{t}_i\|$$

  where $\mathbf{p}_i$ is the touch point and $\mathbf{t}_i$ is the target center for trial i.
- **Tap Task.** *Spread* [38] The 95th percentile diameter of the smallest circle enclosing touch points for a given target. This represents the required button size for reliable selection.
- **Drag Task.** *Throughput* [26] Measures the efficiency of the Drag operation, combining speed and accuracy per Fitts' law.

$$\text{Throughput} = \frac{\log_2\left(\frac{A}{W} + 1\right)}{MT}$$

  where A is the movement amplitude, W is target width, and MT is movement time.
- **Trace Task.** *Movement Error (ME)* [27] The average orthogonal distance between the user's trace and the reference path.

$$ME = \frac{1}{L}\sum_{i=1}^{L} d_i$$

  where d_i is the shortest distance from point i to the reference path.

Table 2. Summary of Significant Task-Performance Results.

Task	Metric	Significant Effect	Statistic	Post-hoc
Tap	Spread	Surface Curvature	$F(3,45) = 3.85$, $p = .016$, $\eta^2 = 0.204$	$R = 45$ mm > $R = 75$ mm (*), Flat (*)
Drag	Throughput	Surface Curvature	$F(3,45) = 3.15$, $p = .034$, $\eta^2 = 0.174$	$R = 60$ mm > $R = 45$ mm (*)
Trace	Movement Error	Surface Curvature	$F(3,45) = 3.37$, $p = .026$, $\eta^2 = 0.184$	$R = 45$ mm > $R = 60$ mm (*)
Trace	Movement Variability	Surface Curvature	$F(3,45) = 3.07$, $p = .037$, $\eta^2 = 0.170$	$R = 45$ mm > $R = 60$ mm (*)

- **Trace Task.** *Movement Variability (MV)* [27] The standard deviation of orthogonal deviation across the trace path. It quantifies consistency in tracing.

$$MV = \sqrt{\frac{1}{L}\sum_{i=1}^{L}(d_i - \bar{d})^2}$$

4.5.2 Behavioral Pattern Metrics.

- **Joint Angle Range.** The angular range of index finger joints (MCP, PIP, DIP) during contact which was captured via motion tracking for each trial.

$$\text{Range}_\theta = \max(\theta) - \min(\theta)$$

- **Wrist Movement Distance.** The accumulated 3D movement distance of the wrist during task execution.

$$D = \sum_{i=2}^{T} \|\mathbf{w}_i - \mathbf{w}_{i-1}\|$$

  where $\mathbf{w}_i$ is the wrist position at frame i.
- **Clutching Count.** The number of clutching actions performed during a single task execution. A clutching action is defined as an intentional lift of the finger from the touch surface, followed by re-contact, used to reposition the finger when the reachable movement range is exceeded.
- **Clutching Distance.** The travel distance of the cursor before each clutching action occurs.

4.5.3 Subjective Evaluation.

- **Raw NASA-TLX [15].** Participants rated six subscales (Mental, Physical, Temporal, Performance, Effort, Frustration) of the condition on a 7-point scale without weighting.
- **Ease of Use & Satisfaction.** Participants answered 7-point Likert-scale questions to rate ease of use and satisfaction.

5 RESULTS

To analyze the data from the study, we used two-way repeated measures ANOVA (RM-ANOVA) for *Surface Curvature* (4 levels) × *Target Distance* (2 levels) in Tap task and three-way RM-ANOVA for *Surface Curvature* (4 levels) × *Cursor Mapping Method* (2 levels) × *Target Distance* (2 levels) in Drag and Trace task. When the data violated normality assumptions, we employed aligned rank transform (ART) before the analysis [7, 49]. We also evaluate sphericity using Mauchley's test and applied Greenhouse–Geisser corrections for violated

Table 3. Summary of Significant Behavioral-Pattern Results in the Drag Task.

Task	Metric	Significant Effect	Statistic	Post-hoc
Drag	PIP Range	Surface Curvature	$F(3, 45) = 10.27$, $p < .001$, $\eta^2 = 0.406$	Flat > R = 45 mm (**), R = 75 mm (**)
Drag	MCP Range	Surface Curvature	$F(3, 45) = 8.81$, $p < .001$, $\eta^2 = 0.370$	R = 60 mm (*), R = 75 mm (*), and Flat (**) > R = 45 mm
Drag	MCP Range	Surface Curvature × Target Distance	$F(1.75, 26.30) = 4.35$, $p = .027$, $\eta^2 = 0.225$	Far : R = 60 mm (*), R = 75 mm (**) > R = 45 mm
Drag	DIP Range	Mapping Method	$F(1, 15) = 12.69$, $p = .003$, $\eta^2 = 0.458$	PM > DM (**)
Drag	DIP Range	Mapping Method × Surface Curvature	$F(1, 15) = 4.96$, $p = .014$, $\eta^2 = 0.249$	R = 45 mm: PM > DM (**)
Drag	Wrist Movement	Surface Curvature	$F(3, 45) = 15.40$, $p < .001$, $\eta^2 = 0.507$	R = 45 mm > R = 60 mm (**), Flat (**)
Drag	Wrist Movement	Surface Curvature × Target Distance	$F(3, 45) = 6.64$, $p < .001$, $\eta^2 = 0.307$	Far : R = 45 mm > R = 60 mm (*), Flat (**)

data. Significant main effects or interactions were followed by a pairwise t-test with Bonferroni correction as a post-hoc test. Effect sizes are reported using partial eta squared (η^2).

During the analysis of results related to the *Cursor Mapping Method*, data under the flat surface was excluded because both mapping methods functioned perfectly identically under a flat surface. The individual effect of Target Distance was not reported as it was unrelated to the subject of this study. Detailed statistically significant results are summarized in Tables 2–5.

5.1 Task Performance

5.1.1 Tap Task. Fig.5 and Table 2 shows the task performance results for the Tap task. *Surface Curvature* showed a significant main effect ($F(3, 45) = 3.85$, $p = .016$, $\eta^2 = 0.204$) for spread. Post-hoc comparisons indicated that the R = 45mm surface resulted in larger spread than both the R = 75mm surface ($p = .036$) and the flat surface ($p = .029$). These effects showed that the higher curvature led to larger tap spread in the experiment. However, no significant effect was observed for the offset.

5.1.2 Drag Task. For the Drag task (Fig. 6, Table 2), Throughput was significantly affected by *Surface Curvature* ($F(3, 45) = 3.15$, $p = .034$, $\eta^2 = 0.174$), with higher Throughput observed at the R = 60mm condition than at the R = 45mm condition. No significant main effects or interactions involving *Cursor Mapping Method* were observed.

5.1.3 Trace Task. For the Trace task (Fig. 7, Table 2)), both Movement Error ($F(3, 45) = 3.37$, $p = .026$, $\eta^2 = 0.184$) and Movement Variance ($F(3, 45) = 3.07$, $p = .037$, $\eta^2 = 0.170$) were significantly affected by *Surface Curvature*. In both measures, the R = 45mm condition showed higher values than the R = 60mm condition. As in the Drag task, no significant effects of *Cursor Mapping Method* were observed.

Table 4. Summary of Significant Behavioral-Pattern Results in the Trace Task.

Task	Metric	Significant Effect	Statistic	Post-hoc
Trace	PIP Range	Surface Curvature	$F(2.03, 30.52) = 12.16$, $p < .001$, $\eta^2 = 0.448$	$R = 75$ mm > $R = 45$ mm (*); Flat > $R = 75$ mm (**), $R = 45$ mm (***)
Trace	MCP Range	Surface Curvature	$F(3, 45) = 4.70$, $p = .006$, $\eta^2 = 0.238$	$R = 75$ mm > $R = 45$ mm (*)
Trace	MCP Range	Surface Curvature × Target Distance	$F(3, 45) = 3.21$, $p = .032$, $\eta^2 = 0.176$	Far : $R = 75$ mm > $R = 45$ mm (*)
Trace	MCP Range	Mapping Method × Surface Curvature	$F(2, 30) = 5.33$, $p = .010$, $\eta^2 = 0.262$	DM: $R = 75$ mm > $R = 45$ mm (**)
Trace	Wrist Movement	Surface Curvature	$F(3, 45) = 28.18$, $p < .001$, $\eta^2 = 0.653$	$R = 45$ mm > $R = 60$ mm (**), $R = 75$ mm (*), Flat (***); $R = 75$ mm > Flat (*)
Trace	Wrist Movement	Surface Curvature × Target Distance	$F(2.03, 30.52) = 16.36$, $p < .001$, $\eta^2 = 0.522$	Near : $R = 45$ mm > $R = 60$ mm (*), $R = 75$ mm (**), Flat (*); Far : $R = 45$ mm > $R = 60$ mm (*), Flat (**)
Trace	Clutching Distance	Surface Curvature	$F(3, 45) = 3.66$, $p = .019$, $\eta^2 = 0.196$	–
Trace	Clutching Distance	Surface Curvature × Target Distance	$F(3, 45) = 7.28$, $p < .001$, $\eta^2 = 0.327$	Near : $R = 75$ mm (*), Flat (***) > $R = 45$ mm
Trace	Clutching Count	Surface Curvature	$F(3, 45) = 3.25$, $p = .030$, $\eta^2 = 0.178$	–
Trace	Clutching Count	Mapping Method	$F(1, 15) = 10.77$, $p = .005$, $\eta^2 = 0.418$	PM > DM (**)
Trace	Clutching Count	Mapping Method × Surface Curvature	$F(2, 30) = 3.58$, $p = .040$, $\eta^2 = 0.193$	–
Trace	Clutching Count	Mapping Method × Target Distance	$F(1, 15) = 8.58$, $p = .010$, $\eta^2 = 0.364$	–

5.2 Behavior Pattern

Hand and finger movement exhibited strong surface curvature-dependent differences during both the Drag (Fig.8,9;Table 3) and Trace (Fig.10, 11;Table 4) tasks.

5.2.1 Drag Task. In the Drag task, movement range (Fig. 8) showed clear curvature-dependent differences. Main effects of *Surface Curvature* were observed in the angle range of PIP ($F(3, 45) = 10.27$, $p < .001$, $\eta^2 = 0.406$) and MCP ($F(3, 45) = 8.81$, $p < .001$, $\eta^2 = 0.370$) joints and in the total movement of the wrist ($F(3, 45) = 15.40$, $p < .001$, $\eta^2 = 0.507$). Post-hoc tests revealed that for both PIP and MCP joints, the range of motion increased as surface curvature decreased, whereas for wrist movement decreased as surface curvature decreased. A significant

Table 5. Summary of Significant Subjective-Evaluation Results.

Measure	**Significant Effect**	**Statistic**	**Post-hoc**
Workload (NASA-TLX)	Mapping Method × Surface Curvature	$F(1.43, 21.47) = 5.75$, $p = .017$, $\eta^2 = 0.277$	PM : $R = 45$ mm > $R = 60$ mm (*), $R = 75$ mm (**)
Workload (NASA-TLX)	Surface Curvature	$F(3, 45) = 6.10$, $p = .001$, $\eta^2 = 0.289$	$R = 45$ mm > $R = 60$ mm (*), $R = 75$ mm (*)
Satisfaction	Surface Curvature	$F(3, 45) = 9.27$, $p < .001$, $\eta^2 = 0.382$	$R = 45$ mm < $R = 60$ mm (*), $R = 75$ mm (*), Flat (*)
Ease of Use	Surface Curvature	$F(3, 45) = 6.44$, $p = .001$, $\eta^2 = 0.300$	$R = 45$ mm < $R = 60$ mm (**), $R = 75$ mm (**), Flat (*)
Ease of Use	Mapping Method × Surface Curvature	$F(2, 30) = 8.81$, $p < .001$, $\eta^2 = 0.370$	PM : $R = 60$ mm (**), $R = 75$ mm (*) > $R = 45$ mm

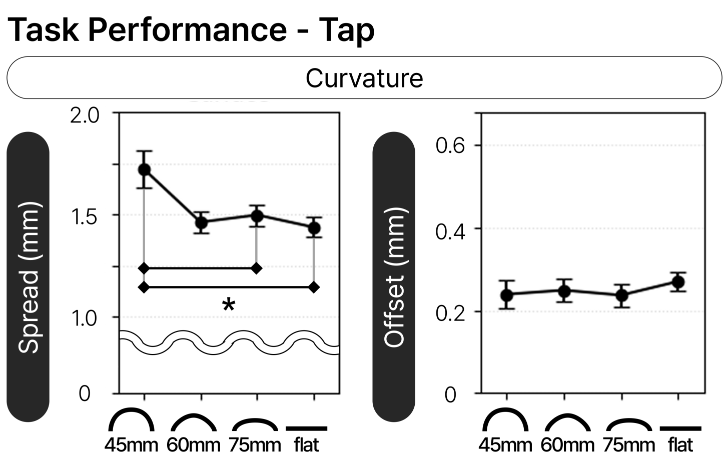

Fig. 5. Results of Spread and Offset of Tap task for *Surface Curvature*. Significant pairwise comparisons are indicated by *(p<.05), **(p< .01), or ***(p< .001). All error bars depict ±standard error.

Surface Curvature × *Target Distance* interaction for wrist movement($F(3, 45) = 6.64$, $p < .001$, $\eta^2 = 0.307$) suggested that wrist movement decreased as surface curvature decreased under the far condition.

For the angle range of MCP joint, a significant *Surface Curvature* × *Target Distance* interaction was also observed ($F(1.75, 26.30) = 4.35$, $p = .027$, $\eta^2 = 0.225$). The post-hoc test suggested that under the far condition, MCP movement increased on lower-curvature surfaces. For the angle range of the DIP joint, the main effect of *Cursor Mapping Method* ($F(1, 15) = 12.69$, $p = .003$, $\eta^2 = 0.458$) and a significant *Cursor Mapping Method* × *Surface Curvature* interaction ($F(1, 15) = 4.96$, $p = .014$, $\eta^2 = 0.249$) were found. Post-hoc test showed that Projection-based Mapping produced a larger DIP angle range than Distance-based Mapping at the $R = 45$mm surface.

No significant effects were found for clutching count and clutching length in the Drag task (Fig. 9).

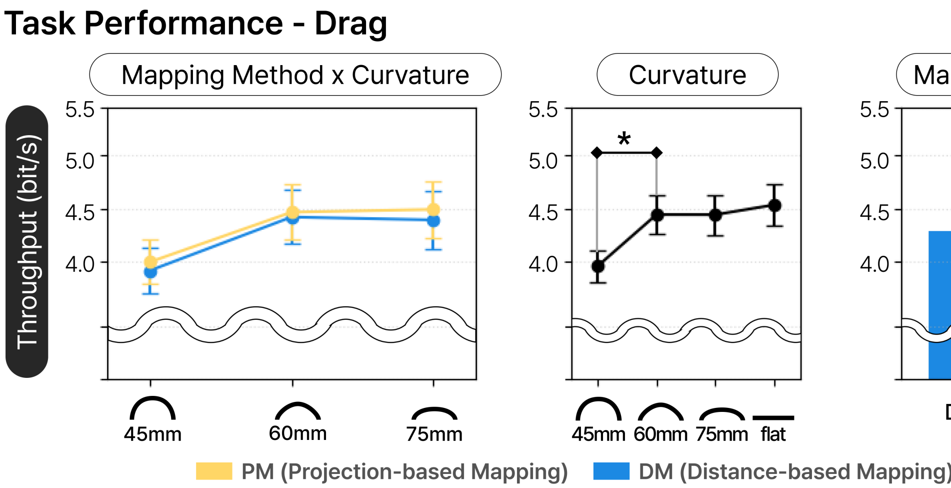

Fig. 6. Result of Throughput of Drag task in various factors. Significant pairwise comparisons are indicated by *(p<.05), **(p< .01), or ***(p< .001). All error bars depict ±standard error.

5.2.2 Trace Task. In the Trace task, movement range (Fig. 10) again showed clear curvature-dependent differences. Main effects of *Surface Curvature* were observed in the angle range of PIP($F(2.03, 30.52) = 12.16$, $p < .001$, $\eta^2 = 0.448$) and MCP($F(3, 45) = 4.70$, $p = .006$, $\eta^2 = 0.238$) joints and in the total movement of the wrist($F(3, 45) = 28.18$, $p < .001$, $\eta^2 = 0.653$). Post-hoc tests revealed that for both finger joints, the range of motion increased as surface curvature decreased, whereas for wrist movement, the range of motion decreased as surface curvature decreased. No significant effects were found for DIP joint movement.

For the angle range of MCP joint, an interaction between *Surface Curvature* × *Target Distance* and *Cursor Mapping Method* × *Surface Curvature* was also found. These interactions suggested that the angle range of the MCP joint increases on lower curvature surfaces under the far condition and the Distance-based Mapping condition, respectively. A significant *Surface Curvature* × *Target Distance* interaction was also observed for wrist movement ($F(2.03, 30.52) = 16.36$, $p < .001$, $\eta^2 = 0.522$). The post-hoc test revealed that, although the degree of change in wrist movement based on curvature varies depending on the target distance, the general trend that movement decreases as surface curvature decreases remains consistent.

Clutching behavior in the Trace task (Fig. 11) also varied across conditions. Clutching distance showed a significant main effect of *Surface Curvature* ($F(3, 45) = 3.66$, $p = .019$, $\eta^2 = 0.196$), although no pairwise comparison reached significance. A significant *Surface Curvature* × *Target Distance* interaction was observed ($F(3, 45) = 7.28$, $p < .001$, $\eta^2 = 0.327$). Post-hoc test results showed that clutching distance increased significantly as surface curvature decreased under the near condition. For clutching count, the main effect of *Cursor Mapping Method* ($F(1, 15) = 10.77$, $p = .005$, $\eta^2 = 0.418$) was found. Post-hoc test suggested that Project-based Mapping resulted in a higher number of clutchings than Distance-based Mapping. Main effects of *Surface Curvature* ($F(3, 45) = 3.25$, $p = .030$, $\eta^2 = 0.178$) and significant interactions of *Cursor Mapping Method* × *Surface Curvature* ($F(2, 30) = 3.58$, $p = .040$, $\eta^2 = 0.193$) and *Cursor Mapping Method* × *Target Distance* ($F(1, 15) = 8.58$, $p = .010$, $\eta^2 = 0.364$) were also found but post-hoc test did not find pairwise differences.

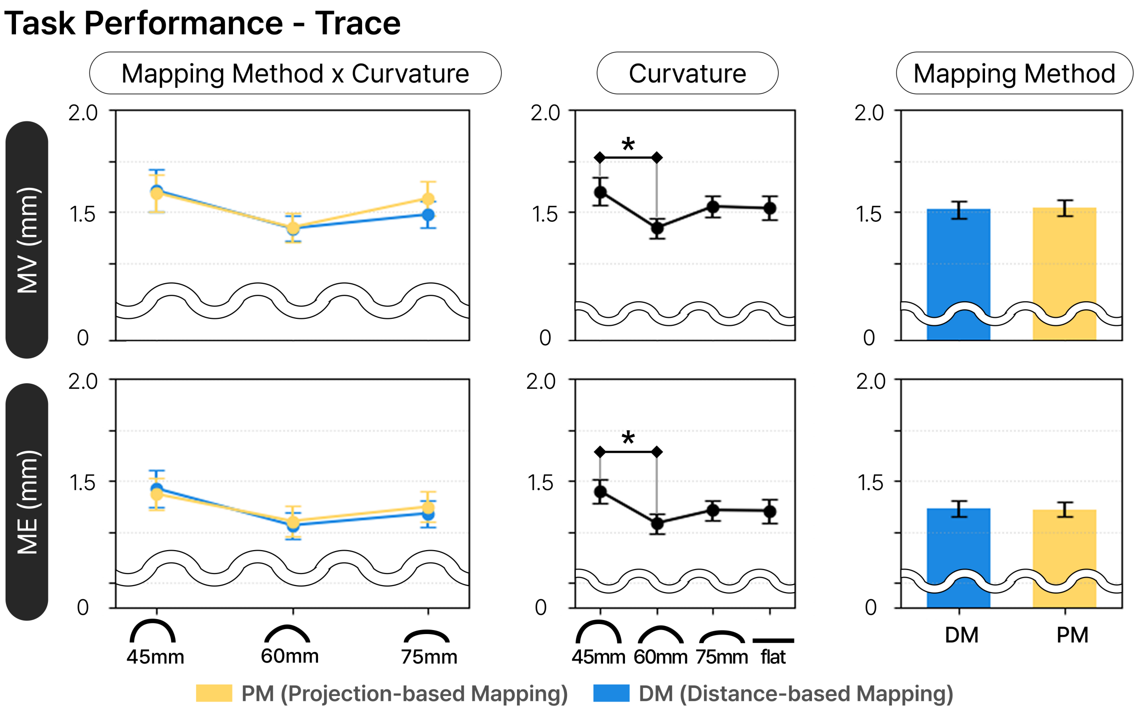

Fig. 7. Result of Movement Variance (MV) and Movement Error (ME) of Trace task in various factors. Significant pairwise comparisons are indicated by *(p<.05), **(p< .01), or ***(p< .001). All error bars depict ±standard error.

5.3 Subjective Evaluation

Subjective evaluation result revealed consistent differences in usability and preference across surface curvature and cursor mapping conditions (Fig. 12, Table 5).

5.3.1 Workload. For overall workload (raw NASA-TLX), *Surface Curvature* showed a significant main effect on workload ($F(3, 45) = 6.10$, $p = .001$, $\eta^2 = 0.289$). Post-hoc tests suggested that surfaces with the highest curvature result in a higher workload than other curved surfaces. A significant interaction between *Cursor Mapping Method* and *Surface Curvature* ($F(1.43, 21.47) = 5.75$, $p = .017$, $\eta^2 = 0.277$) indicated that such a tendency occurs under the Projection-based method.

5.3.2 Satisfaction and Ease of Use. Both Satisfaction ($F(3, 45) = 9.27$, $p < .001$, $\eta^2 = 0.382$) and Ease of Use ($F(3, 45) = 6.44$, $p = .001$, $\eta^2 = 0.300$) showed a significant main effect of *Surface Curvature*. Post-hoc test results showed that the $R = 45$mm surface had significantly lower scores for both Satisfaction and Ease of Use compared to other surfaces.

A significant *Cursor Mapping Method* × *Surface Curvature* interaction was found for Ease of Use ($F(2, 30) = 8.81$, $p < .001$, $\eta^2 = 0.370$). Within the projection-based method, the $R = 45$mm surface was found to be more difficult to use than other curved surfaces.

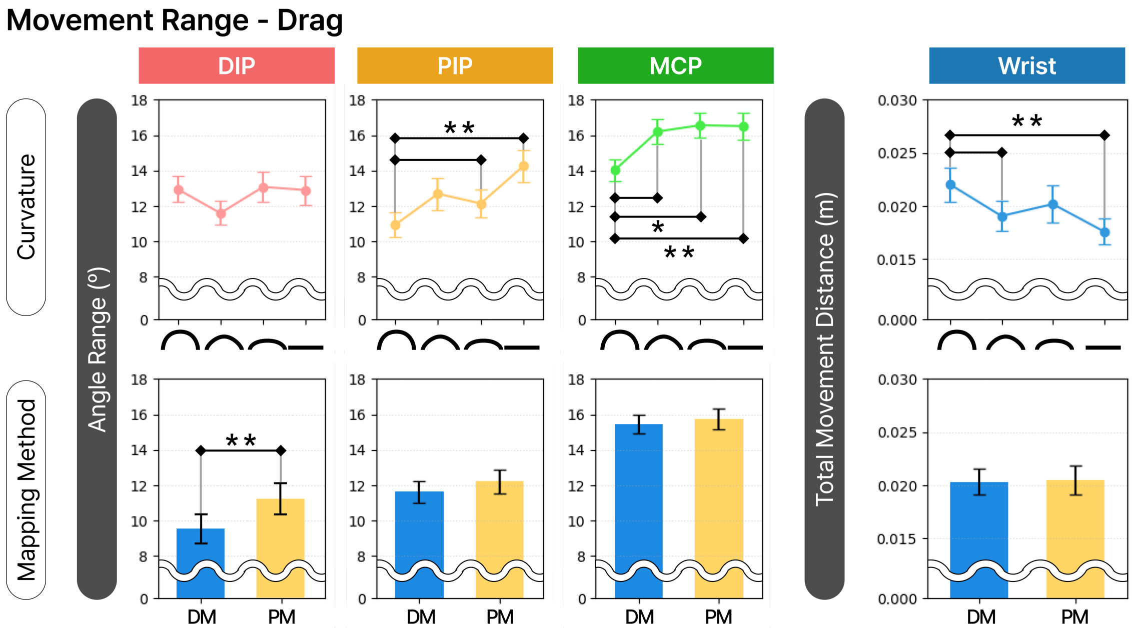

Fig. 8. Movement range data segmented by *Surface Curvature* and *Cursor Mapping Method* for Drag task. Significant pairwise comparisons are indicated by *(p<.05), **(p< .01), or ***(p< .001). All error bars depict ±standard error.

6 DISCUSSION

6.1 Effect of Surface Curvature

Surface curvature had a substantial impact on user's behavioral pattern, task performance, and perceived usability.

Behavior Pattern Our analysis of finger joint articulation and wrist motion during the Drag and Trace tasks revealed a consistent effect of surface curvature. As curvature increased, the range of motion of the finger joints decreased, whereas wrist movement increased across both tasks. This pattern suggests that users adopted different movement strategies depending on surface curvature(Fig. 13).

Under high curvature conditions, participants tended to keep their fingers extended and relatively fixed, moving the hand as a whole to perform input. This strategy can be interpreted as an attempt to maintain the orientation of the contact plane between the fingertip and the surface parallel to the surface normal, thereby enhancing input stability. In contrast, on gently curved surfaces, the orientation of the contact plane remains relatively consistent regardless of hand position. As a result, participants were less required to actively align their hand orientation, allowing them to minimize whole-hand motion and rely primarily on finger joint articulation. This strategy likely reduced physical effort and task load.

Differences in movement strategies across curvature conditions were also reflected in clutching behavior. In the Drag task, where target distances were short and trajectories were linear, no significant effects of curvature were observed, as clutching was rarely required. In contrast, the Trace task exhibited a significant interaction between surface curvature and target distance, yielding two key insights.

First, the maximum distance that users could traverse stably in a single motion increased as surface curvature decreased. In the Near condition, the average number of clutches remained below two across all curvature levels,

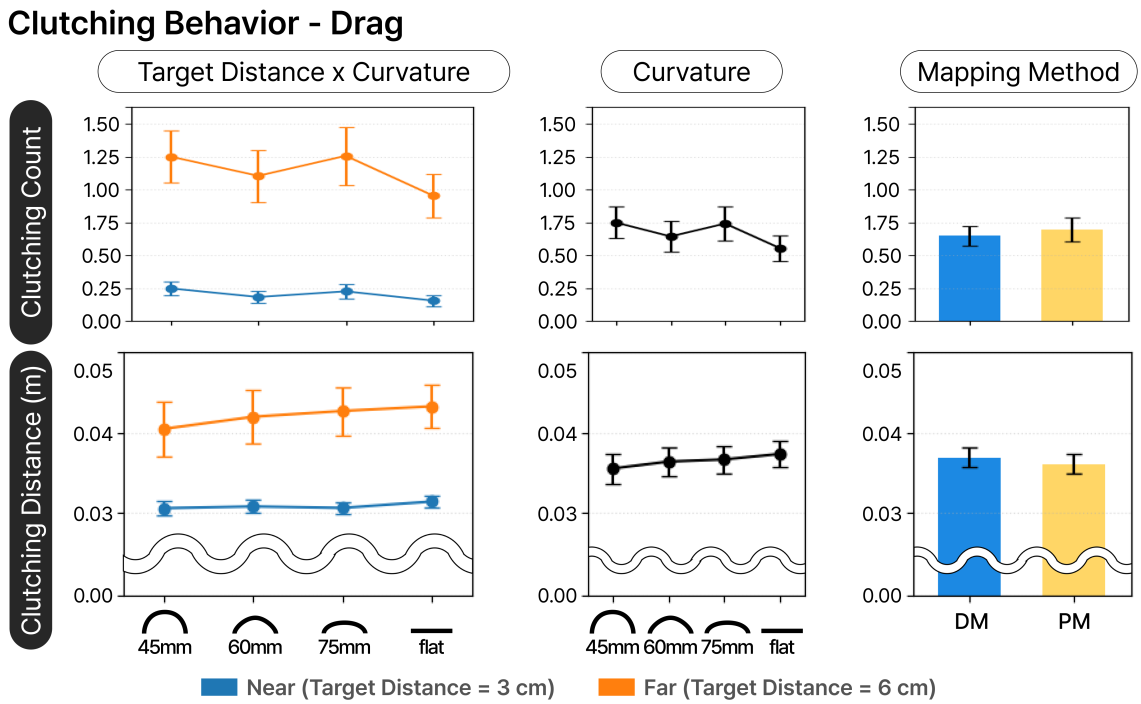

Fig. 9. Clutching behavior data segmented by various factor for Drag task. Significant pairwise comparisons are indicated by *(p<.05), **(p< .01), or ***(p< .001). All error bars depict ±standard error.

indicating that participants attempted to complete the task with a single continuous movement whenever possible. Notably, the clutching distance in this condition increased significantly with decreasing curvature, suggesting that lower curvature enables a longer stable movement range.

Second, users exhibited different clutching strategies depending on curvature. In indirect touch scenarios where the users don't see their hand and surface during interaction, increasing curvature makes it more difficult for users to estimate the spatial relationship between the fingertip and the surface when the hand is lifted. Consequently, repositioning the finger incurs a higher cognitive cost on the high curvature condition. Therefore, participants appeared to move their cursor as far as they could stably travel in a single motion, regardless of the required target distance. On the flat surface, however, users approached clutching differently depending on the target distance. They avoided clutching intentionally for Near conditions, but actively utilized clutching at Far conditions, dividing input into shorter segments. This is observed in the fact that the average clutching distance under Near conditions is approximately twice that under Far conditions on flat surfaces. In summary, on low curvature surfaces, participants flexibly integrated clutching as part of their input strategy, while on high curvature surfaces, they showed reduced flexibility in clutching behavior. This tendency explains why the difference in clutching distance based on target distance tends to decrease as curvature increases.

When these two effects, which have opposite influences on the clutching count, are combined, the overall clutching count showed no difference based on curvature.

Task Performance A significant performance degradation was observed only at the highest curvature condition (R = 45mm) across all tasks. No significant differences were found among the remaining curvature

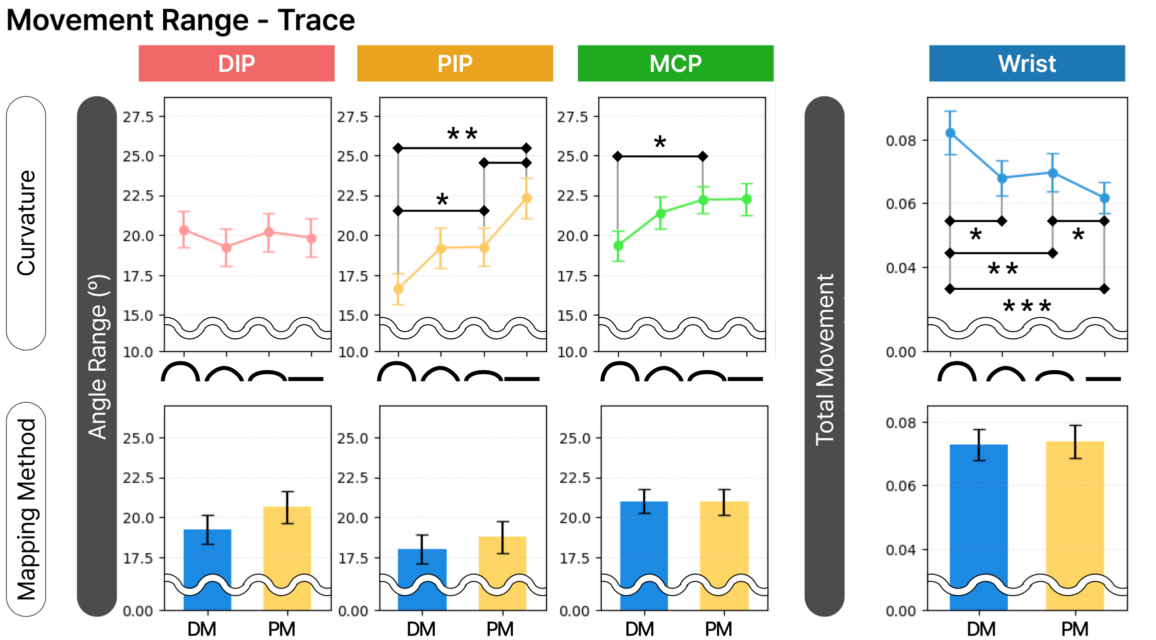

Fig. 10. Movement range data segmented by *Surface Curvature* and *Cursor Mapping Method* for Trace task. Significant pairwise comparisons are indicated by *(p<.05), **(p< .01), or ***(p< .001). All error bars depict ±standard error.

levels. These results suggest that performance degradation became most evident at the highest curvature condition (R = 45mm), whereas the lower curvature conditions tested here remained closer to the flat baseline.

A particularly notable finding emerged when comparing our results for the spread in the tap task with prior work on direct touch interaction on similar convex hemispherical surfaces. Prior work [38] reported that, in direct touch on convex curved surfaces, spread decreased as curvature increased. The authors explained this result by suggesting that users can adjust finger posture, thereby reducing fingertip contact area on a higher curvature surface during tapping and achieving higher precision. In contrast, in the indirect-touch condition examined in this study, spread showed the opposite tendency, increasing as curvature increased(Fig. 14).

We believe that this discrepancy can be explained by the curvature-dependent behavior pattern changes in the indirect touch scenario observed in our study. In direct touch scenarios, a previous study attributed the reduced spread on highly curved surfaces to a smaller contact area between the fingertip and the surface. However, this assumes that users can freely adjust finger posture to minimize contact area during target acquisition. [38] In an indirect touch scenario, users tend to maintain a fixed finger posture and rely on whole-hand motion under high curvature conditions as observed in our behavioral pattern analysis. Thus, users may poke targets with a precision-oriented finger posture on lower curvature surfaces, but they press targets with a fixed posture on higher curvature surfaces, leading to a larger contact area between the fingertip and the surface.

Consequently, larger effective target sizes may be needed as surface curvature increases in indirect touch scenarios, in contrast to prior findings for direct touch scenarios. This result also suggests that design guidelines derived from direct touch curved interfaces may not directly apply to indirect touch interaction in XR environments.

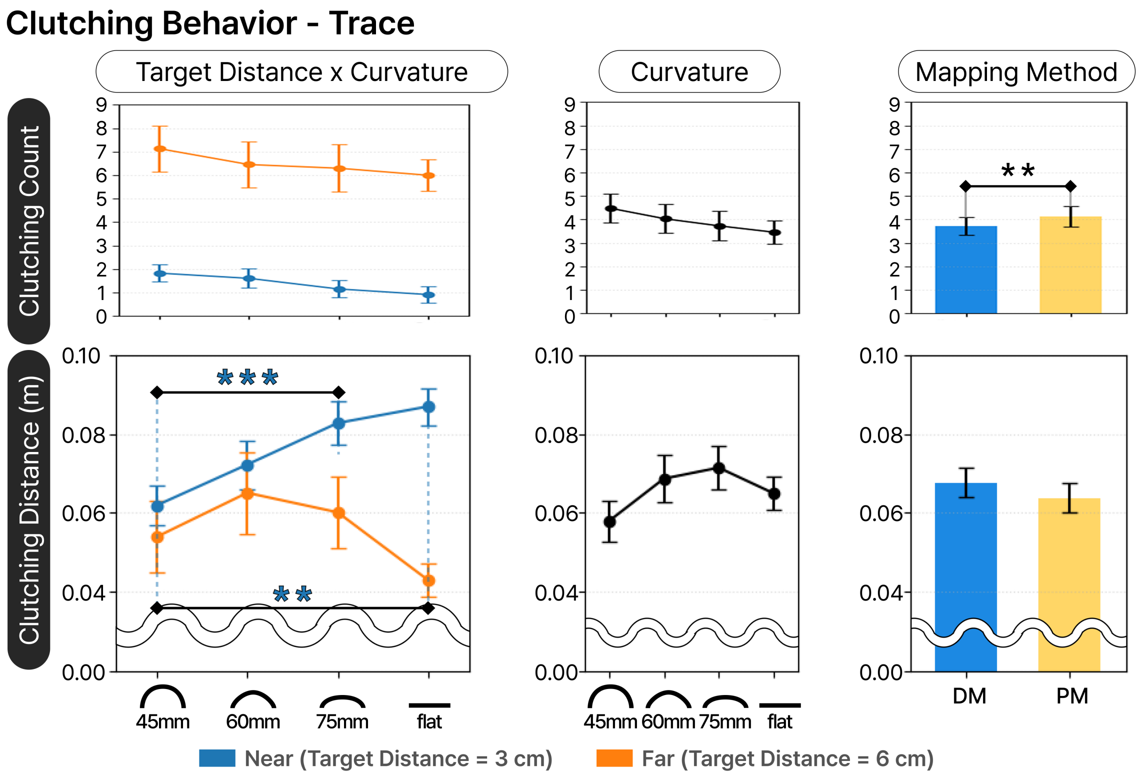

Fig. 11. Clutching behavior data segmented by various factor for Trace task. Significant pairwise comparisons are indicated by *(p<.05), **(p< .01), or ***(p< .001). All error bars depict ±standard error.

Subjective Evaluation Surface curvature also had a pronounced effect on perceived usability. The results indicate that the highest curvature condition ($R = 45$mm) led to significantly higher workload and lower satisfaction and ease-of-use ratings compared to all other conditions. No significant differences were observed among the remaining curved surfaces ($R = 60$mm, $R = 75$mm) and the flat condition. These findings align with the performance results and suggest that the lower curvature conditions tested here were comparable to the flat condition contrary to highest curvature condition, from both objective and subjective perspectives.

6.2 Effect of Cursor Mapping Method

Compared to surface curvature, the effects of the cursor mapping method were relatively limited. No significant performance or subject usability differences were found in the Drag and Trace tasks.

Subjective usability measures did not reveal a clear main effect of the mapping method. Differences in workload and Ease of Use appeared only in specific contexts, which are further discussed in terms of interaction effects with surface curvature. Overall, these results suggest that the cursor mapping method does not exert a strong independent influence on task performance or general usability, and that neither perceptual model is universally dominant across curvature conditions.

Behavior pattern metrics showed similarly limited effects. Only the range of motion of the DIP joint in the Drag task differed significantly between mapping methods, while no significant differences were observed for

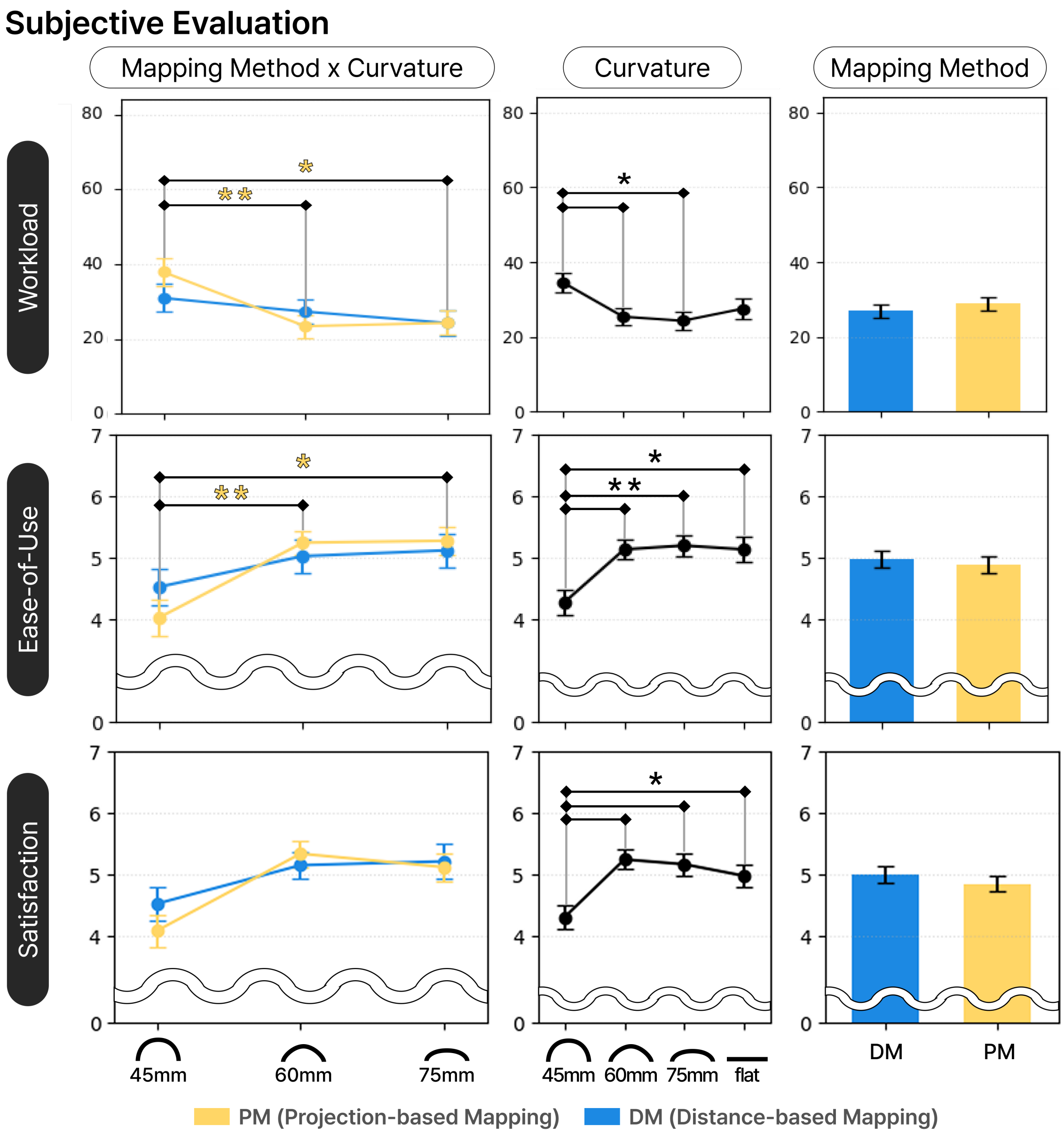

Fig. 12. Subjective evaluation results, illustrating users' perceived Workload, Ease of Use, and Satisfaction. Clutching behavior data segmented by various factors. Significant pairwise comparisons are indicated by * (p<.05), ** (p< .01), or *** (p< .001). All error bars depict ±standard error.

other joints or wrist motion. The only statistically significant result in the clutching-related metrics was that the number of clutches was higher when using the Projection-based Mapping in the Trace task compared to

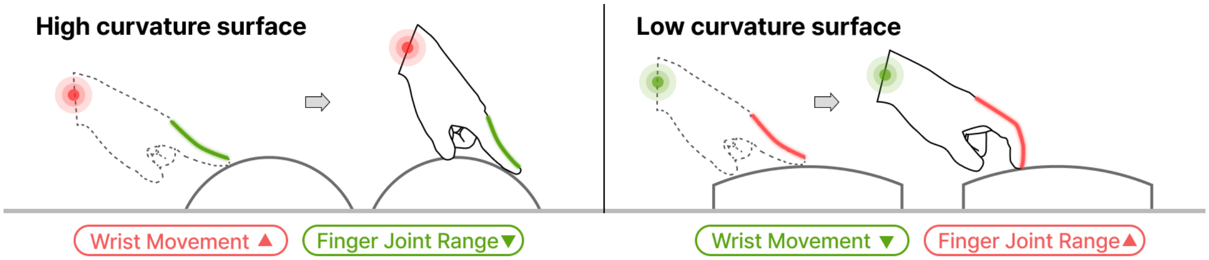

Fig. 13. Input strategy users employ change depending on surface curvature. On high curvature surfaces, users perform input by moving their entire hand while keeping their fingers in a stretched, fixed position. Conversely, on low curvature surfaces, input is performed by utilizing finger joints while minimizing overall hand movement.

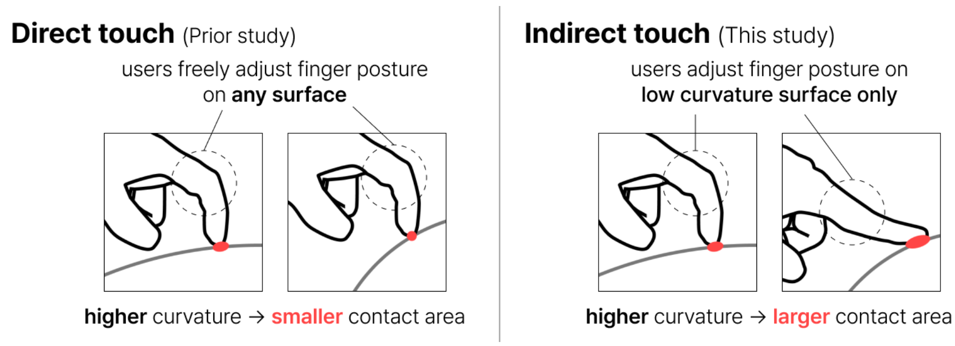

Fig. 14. In direct touch, users can freely adjust their finger posture to reduce contact area as curvature increases. In contrast, indirect touch fixes finger posture under high curvature conditions, relying instead on whole-hand movement, which increases contact area. Thus, unlike direct touch, the Tap spread, which represents the minimum button size, increases as surface curvature increases in indirect touch scenarios.

the Distance-based Mapping. This is because the Projection-based Method causes the cursor to move a shorter distance for the same amount of finger movement, which may require users to perform more clutching.

6.3 Interaction between Surface Curvature and Mapping Method

Although no significant interaction effects between surface curvature and mapping method were found for performance metrics, such interactions emerged in both behavioral pattern and subjective usability measures. For example, in the Drag task under the $R = 45$mm condition, the Projection-based Mapping resulted in increased DIP joint motion. In the Trace task, an interaction effect was observed in the MCP movement range. Generally, as curvature increased, MCP movement decreased. However, this decrease was less pronounced when using Projection-based mapping. It suggests that using Projection-based Mapping on high curvature surfaces may require additional movement compared to Distance-based Mapping.

Subjective evaluations were consistent with these behavioral patterns. Significant interactions between surface curvature and cursor mapping method were observed for Ease-of-use and workload ratings. When using Projection-based Mapping, the workload increased significantly, and ease of use decreased as curvature increased, but when using Distance-based Mapping, there was no significant usability decrement based on surface curvature.

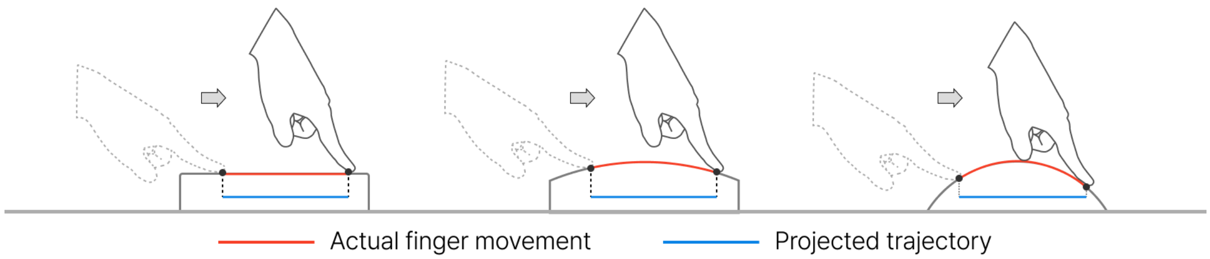

Fig. 15. In the Projection-based Method, as surface curvature increases, the finger moves along a 3D path following the curved surface (red), but cursor movement is determined based on the trajectory projected onto a plane (blue). This causes the geometric mismatch between the actual distance traveled by the finger and the amount the cursor moves to grow as curvature increases.

These results suggest that Projection-based Mapping may amplify both visual distortion and motor mismatch in highly curved environments, thereby degrading user experience (Fig. 15).

In summary, interaction effects between surface curvature and cursor mapping method were primarily observed in behavioral patterns and subjective usability rather than task performance. Projection-based mapping resulted in reduced usability and increased motion range on high curvature surfaces, whereas distance-based mapping did not show the same usability decrement based on surface curvature.

7 DESIGN GUIDELINE AND APPLICATIONS

7.1 Design Guideline

Based on the findings of this study, we propose a set of design guidelines for indirect touch interaction on curved surfaces in XR environments. For most performance and usability metrics, the results generally fell into two groups: the highest curvature condition ($R = 45$mm) and the low curvature conditions ($R = 60$mm, 75mm, ∞). Accordingly, in the following guidelines, we refer to these two groups as high curvature surfaces ($R \leq 45$ mm) and low curvature surfaces ($R \geq 60$ mm).

(1) **Interaction Type** On low curvature surfaces, users primarily articulate finger joints to drive cursor movement, enabling precise interaction with relatively low physical effort. In high curvature cases, users keep the finger posture relatively fixed and instead rely on whole-hand motion to maintain stable contact, thereby increasing the physical workload.
Therefore, high curvature surfaces are may be better suited to simple and short interactions, such as confirmation or undo. Interactions that require precision or prolonged use may be placed on low curvature surfaces.

(2) **Button Size** The effect of curvature on button size differs between direct and indirect touch. Prior work on direct touch on curved displays reports that higher curvature reduces fingertip–surface contact area. That is, as the surface curvature increases, the minimum button size decreases. However, the opposite trend was observed in our indirect touch situations. Since users cannot visually perceive the physical surface, they adopt different motion strategies depending on curvature. They rely on finger joint movements to perform precise taps on low curvature surfaces, while maintaining a fixed finger posture on high curvature surfaces. Consequently, the effective contact area appears to increase with curvature in our indirect touch scenario. Therefore, larger buttons may be needed on highly curved surfaces for indirect touch. For direct touch, prior work suggests a different trend.

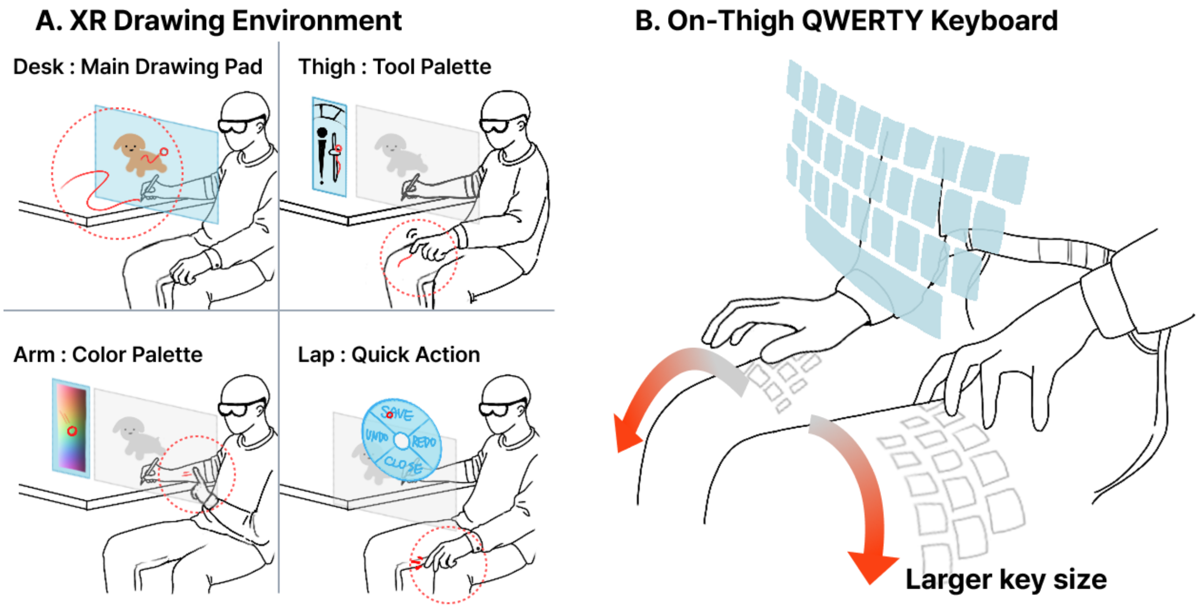

Fig. 16. Application examples of the curved-surface touch design guidelines. (a) XR drawing environment distributing interface elements across multiple everyday surfaces with different curvature characteristics. Flat and mildly curved surfaces support precise and continuous interactions, while steeply curved surfaces are reserved for simple, quick actions and use distance-based cursor mapping. (b) On-thigh QWERTY keyboard for indirect touch input, where key size increases toward regions with higher surface curvature to compensate for reduced tapping precision.

(3) **Interaction Area** Repositioning the finger induces a higher cognitive load on high curvature surfaces than low curvature surfaces. It makes users may become less willing to rely on clutching flexibly. They instead attempt to move as far as possible within a single stable reach. Therefore, it may be beneficial to keep the interaction area relatively small where the cursor moves to a small region when the interface controlled by high curvature surfaces. This allows users to maintain stability while using the interface without clutching. On low curvature surfaces, users can freely utilize clutching and comfortably cover a wider area, enabling support for a larger interaction area.

(4) **Cursor Mapping Method** In the case of distance-based mapping, there was no difference in usability based on surface curvature, but in the case of projection-based mapping, significant differences in usability were observed depending on curvature. Projection-based mapping worked effectively on planar and low curvature surfaces. Yet on high curvature surfaces, the workload increased due to discrepancies between visual feedback and proprioceptive cues. Distance-based mapping reduces this mismatch and maintains the usability on high curvature surfaces. Therefore, distance-based cursor mapping may be a better option for high curvature surfaces.

7.2 Application

This section presents illustrative example interfaces that apply our proposed design guidelines to touch interaction on curved everyday surfaces in XR. These examples demonstrate how design choices, such as interaction type, button size, interaction area, and cursor mapping, can be informed by practical interface guidelines.

These application examples are intended to illustrate conceptual examples based on current research findings rather than serving as empirically validated interface guidelines for actual body parts. In this section, we arbitrarily assumed the thigh to be a “low-curvature surface” and the knee or forearm to be a “high-curvature surface” to demonstrate actual interface design guidelines; however, further verification is needed to determine what type of surface these areas actually correspond to.

7.2.1 XR Drawing Environment. The first example considers an XR drawing environment (Fig. 16-A). The interface is distributed across multiple physical surfaces with varying curvature characteristics.

A flat surface (e.g., a desk) is used as the main drawing pad, because it supports finger-based input with high precision and low physical effort. This surface supports continuous and fine-grained interactions such as drawing and tracing. In this conceptual example, a low-curvature body-related surface such as the thigh is used for tool selection and parameter adjustment. It requires moderate precision, but the interaction frequency is lower than that of a sketch plane. A moderately curved body-related surface, such as the arm, can be used for the color palette with distance-based mapping. A more highly curved body-related surface, such as around the knee, is reserved for simple and short interactions such as quick actions (e.g., save, undo/redo, exit). As experimental results indicate that high curvature constrains finger articulation and induces whole-hand movement with increased workload, these surfaces are utilized for simple essential interactions.

This interface layout demonstrates how interaction complexity can be gradually reduced as surface curvature increases, while the cursor mapping strategy is adapted to maintain usability.

7.2.2 On-Thigh QWERTY Keyboard. The second example illustrates a on-the-thigh QWERTY keyboard designed for text entry in situations where a desk is unavailable, such as while seated on public transportation (Fig. 16-B).

The keyboard primarily occupies the central region of both thighs, which is treated as a relatively lower-curvature area. In that area, finger joint movement is relatively free, allowing for long-term and precise input. Therefore, this area is suitable for interactions requiring prolonged use, such as typing. The interface curvature may increase toward the outer regions of the thighs. Thus, the key size is gradually enlarged to compensate for reduced tapping precision. This design reflects the finding that higher curvature leads to increased tap spread in indirect touch scenarios.

8 LIMITATIONS AND FUTURE WORK

The effective curvature of non-spherical curved surfaces varies continuously depending on the direction of the user’s movement, including cylindrical geometries. Since users’ input directions and movement strategies dynamically evolve during task execution in indirect touch, it becomes difficult to isolate curvature effects as an independent variable. For this reason, we chose spherical surfaces with uniform curvature in all directions as the experimental substrate in this study.

Although this design choice is an intentional simplification for systematic control, many real-world surfaces, including the human body, are closer to cylindrical or asymmetric geometries than spherical ones. As a result, this study does not fully capture the diversity of curved surfaces encountered in everyday interaction. Future work should therefore extend the study’s scope beyond surface curvature to include surface shape. Examining cylindrical and asymmetric surfaces may reveal additional constraints and interaction strategies that are not observable under uniform spherical curvature.

Another limitation lies in the experimental setup used for touch detection and touch-point estimation. To ensure robust real-time touch event detection across all surface conditions, we used capacitive sensing, while touch location was approximated from the marker’s position attached above the participant’s index fingernail at the moment of contact. As a result, the setup constrained the interaction primarily to single-finger touch and did not allow us to examine more natural contact strategies, such as resting the thumb or another finger on the surface for stabilization during continuous input, or multi-touch interaction. In addition, since the touch location was estimated indirectly from the fingernail marker position. This may have introduced a mismatch between the measured and actual touch locations, particularly when finger posture or contact angle varied across curvature conditions. Future work should investigate curved-surface interaction using sensing approaches that more directly capture the contact point and allow a wider range of natural hand postures.

In addition, as this study assumes that any everyday surface can serve as an input surface in XR, the user's posture based on various surface positions remains an important factor for further exploration. In this study, participants engaged in interactions while seated at a desk and using curved surfaces parallel to the ground. It would be valuable to investigate how curvature effects change when users are standing or when surfaces are oriented vertically relative to the ground. Comparing such conditions could provide further insights into how surface geometry, body posture, and input strategies jointly affect indirect touch interaction in XR environments.

9 CONCLUSION

We investigated how surface curvature and cursor-mapping strategies influence user performance, behavioral patterns, and usability in indirect touch interaction for XR environments. Surface curvature plays a central role in shaping task performance and usability across task types. In particular, we found that the curvature threshold exists between $R = 45$mm and $R = 60$mm, where pronounced performance degradation and reduced usability emerged. In contrast, under milder curvature conditions (R ≤ 60mm), task performance, usability and behavioral characteristics remained comparable to those on flat surfaces. Surface curvature also changes users' input strategies. On flat and mildly curved surfaces, users relied on finger joint movement to perform input. As curvature increased, however, users adopted whole-hand movement strategies to maintain stable contact. The effect of the cursor mapping method was observed when it was combined with surface curvature. Under high curvature conditions, the Distance-based mapping supported more stable and consistent input than the Projection-based mapping. The design guidelines derived from this study provide an initial empirical basis for developing more ergonomic and robust XR indirect touch interfaces for curved surfaces.

Acknowledgments

This work was supported by the IITP(Institute of Information & Communications Technology Planning & Evaluation)-ITRC(Information Technology Research Center) grant funded by the Korea government(Ministry of Science and ICT)(IITP-2026-RS-2024-00436398).

References

[1] Felipe Bacim, Mike Sinclair, and Hrvoje Benko. 2013. Understanding touch selection accuracy on flat and hemispherical deformable surfaces. In *Proceedings of Graphics Interface 2013* (Regina, Sascatchewan, Canada) *(GI '13)*. Canadian Information Processing Society, CAN, 197–204.

[2] Hrvoje Benko. 2009. Beyond flat surface computing: challenges of depth-aware and curved interfaces. In *Proceedings of the 17th ACM International Conference on Multimedia* (Beijing, China) *(MM '09)*. Association for Computing Machinery, New York, NY, USA, 935–944. doi:10.1145/1631272.1631462

[3] Joanna Bergström and Kasper Hornbæk. 2019. Human–Computer Interaction on the Skin. *ACM Comput. Surv.* 52, 4, Article 77 (Aug. 2019), 14 pages. doi:10.1145/3332166

[4] Li-Wei Chan, Hui-Shan Kao, Mike Y. Chen, Ming-Sui Lee, Jane Hsu, and Yi-Ping Hung. 2010. Touching the void: direct-touch interaction for intangible displays. In *Proceedings of the SIGCHI Conference on Human Factors in Computing Systems* (Atlanta, Georgia, USA) *(CHI '10)*. Association for Computing Machinery, New York, NY, USA, 2625–2634. doi:10.1145/1753326.1753725

[5] Niloofar Dezfuli, Mohammadreza Khalilbeigi, Jochen Huber, Murat Özkorkmaz, and Max Mühlhäuser. 2014. PalmRC: leveraging the palm surface as an imaginary eyes-free television remote control. *Behaviour & Information Technology* 33, 8 (2014), 829–843. arXiv:https://doi.org/10.1080/0144929X.2013.810781 doi:10.1080/0144929X.2013.810781

[6] Camille Dupré, Caroline Appert, Stéphanie Rey, Houssem Saidi, and Emmanuel Pietriga. 2024. TriPad: Touch Input in AR on Ordinary Surfaces with Hand Tracking Only. In *Proceedings of the 2024 CHI Conference on Human Factors in Computing Systems*. 1–18.

[7] Lisa A. Elkin, Matthew Kay, James J. Higgins, and Jacob O. Wobbrock. 2021. An Aligned Rank Transform Procedure for Multifactor Contrast Tests. In *The 34th Annual ACM Symposium on User Interface Software and Technology* (Virtual Event, USA) *(UIST '21)*. Association for Computing Machinery, New York, NY, USA, 754–768. doi:10.1145/3472749.3474784
[8] Chuhan Gao, Xinyu Zhang, and Suman Banerjee. 2018. Conductive Inkjet Printed Passive 2D TrackPad for VR Interaction. In *Proceedings of the 24th Annual International Conference on Mobile Computing and Networking* (New Delhi, India) *(MobiCom '18)*. Association for Computing Machinery, New York, NY, USA, 83–98. doi:10.1145/3241539.3241546
[9] Hyunjae Gil, Ashish Pratap, Iniyan Joseph, and Jin Ryong Kim. 2025. PropType: Everyday Props as Typing Surfaces in Augmented Reality. In *Proceedings of the 2025 CHI Conference on Human Factors in Computing Systems (CHI '25)*. Association for Computing Machinery, New York, NY, USA, Article 730, 18 pages. doi:10.1145/3706598.3714056
[10] Patrick Grady, Jeremy A. Collins, Chengcheng Tang, Christopher D. Twigg, Kunal Aneja, James Hays, and Charles C. Kemp. 2024. PressureVision++: Estimating Fingertip Pressure from Diverse RGB Images. In *2024 IEEE/CVF Winter Conference on Applications of Computer Vision (WACV)*. 8683–8693. doi:10.1109/WACV57701.2024.00850
[11] Patrick Grady, Chengcheng Tang, Samarth Brahmbhatt, Christopher D. Twigg, Chengde Wan, James Hays, and Charles C. Kemp. 2022. PressureVision: Estimating Hand Pressure fromnbsp;anbsp;Single RGB Image. In *Computer Vision – ECCV 2022: 17th European Conference, Tel Aviv, Israel, October 23–27, 2022, Proceedings, Part VI* (Tel Aviv, Israel). Springer-Verlag, Berlin, Heidelberg, 328–345. doi:10.1007/978-3-031-20068-7_19
[12] Dustin T. Han, Mohamed Suhail, and Eric D. Ragan. 2018. Evaluating Remapped Physical Reach for Hand Interactions with Passive Haptics in Virtual Reality. *IEEE Transactions on Visualization and Computer Graphics* 24, 4 (2018), 1467–1476. doi:10.1109/TVCG.2018.2794659
[13] Chris Harrison, Hrvoje Benko, and Andrew D. Wilson. 2011. OmniTouch: wearable multitouch interaction everywhere. In *Proceedings of the 24th Annual ACM Symposium on User Interface Software and Technology* (Santa Barbara, California, USA) *(UIST '11)*. Association for Computing Machinery, New York, NY, USA, 441–450. doi:10.1145/2047196.2047255
[14] Chris Harrison, Desney Tan, and Dan Morris. 2010. Skinput: appropriating the body as an input surface. In *Proceedings of the SIGCHI Conference on Human Factors in Computing Systems* (Atlanta, Georgia, USA) *(CHI '10)*. Association for Computing Machinery, New York, NY, USA, 453–462. doi:10.1145/1753326.1753394
[15] Sandra G Hart and Lowell E Staveland. 1988. Development of NASA-TLX (Task Load Index): Results of empirical and theoretical research. In *Advances in psychology*. Vol. 52. Elsevier, 139–183.
[16] Hayati Havlucu, Mehmet Yarkın Ergin, İdil Bostan, Oğuz Turan Buruk, Tilbe Göksun, and Oğuzhan Özcan. 2017. It Made More Sense: Comparison of User-Elicited On-skin Touch and Freehand Gesture Sets. In *Distributed, Ambient and Pervasive Interactions*, Norbert Streitz and Panos Markopoulos (Eds.). Springer International Publishing, Cham, 159–171.
[17] Fengming He, Xiyun Hu, Jingyu Shi, Xun Qian, Tianyi Wang, and Karthik Ramani. 2023. Ubi Edge: Authoring Edge-Based Opportunistic Tangible User Interfaces in Augmented Reality. In *Proceedings of the 2023 CHI Conference on Human Factors in Computing Systems* (Hamburg, Germany) *(CHI '23)*. Association for Computing Machinery, New York, NY, USA, Article 461, 14 pages. doi:10.1145/3544548.3580704
[18] Juan David Hincapié-Ramos, Xiang Guo, Paymahn Moghadasian, and Pourang Irani. 2014. Consumed endurance: a metric to quantify arm fatigue of mid-air interactions. In *Proceedings of the SIGCHI Conference on Human Factors in Computing Systems* (Toronto, Ontario, Canada) *(CHI '14)*. Association for Computing Machinery, New York, NY, USA, 1063–1072. doi:10.1145/2556288.2557130
[19] Da-Yuan Huang, Liwei Chan, Shuo Yang, Fan Wang, Rong-Hao Liang, De-Nian Yang, Yi-Ping Hung, and Bing-Yu Chen. 2016. DigitSpace: Designing Thumb-to-Fingers Touch Interfaces for One-Handed and Eyes-Free Interactions. In *Proceedings of the 2016 CHI Conference on Human Factors in Computing Systems* (San Jose, California, USA) *(CHI '16)*. Association for Computing Machinery, New York, NY, USA, 1526–1537. doi:10.1145/2858036.2858483
[20] Per Jenmalm, Seth Dahlstedt, and Roland S. Johansson. 2000. Visual and Tactile Information About Object-Curvature Control Fingertip Forces and Grasp Kinematics in Human Dexterous Manipulation. *Journal of Neurophysiology* 84, 6 (2000), 2984–2997. arXiv:https://doi.org/10.1152/jn.2000.84.6.2984 doi:10.1152/jn.2000.84.6.2984 PMID: 11110826.
[21] Jina Kim, Minyung Kim, Woo Suk Lee, and Sang Ho Yoon. 2023. VibAware: Context-Aware Tap and Swipe Gestures Using Bio-Acoustic Sensing. In *Proceedings of the 2023 ACM Symposium on Spatial User Interaction*. 1–12.
[22] Jina Kim, Yang Zhang, and Sang Ho Yoon. 2025. T2IRay: Design of Thumb-to-Index based Indirect Pointing for Continuous and Robust AR/VR Input. In *Proceedings of the 2025 CHI Conference on Human Factors in Computing Systems (CHI '25)*. Association for Computing Machinery, New York, NY, USA, Article 854, 16 pages. doi:10.1145/3706598.3713442
[23] Katerina Koleva, Martin Hedlund, Gunilla Berndtsson, Martin Ek, Héctor Caltenco, and Andrii Matviienko. 2025. KnuckleBoard: Knuckle-based Input in Augmented Reality while Sitting, Standing, and Walking. In *Proceedings of the Extended Abstracts of the CHI Conference on Human Factors in Computing Systems (CHI EA '25)*. Association for Computing Machinery, New York, NY, USA, Article 366, 8 pages. doi:10.1145/3706599.3720281

[24] Chen Liang, Xutong Wang, Zisu Li, Chi Hsia, Mingming Fan, Chun Yu, and Yuanchun Shi. 2023. ShadowTouch: Enabling Free-Form Touch-Based Hand-to-Surface Interaction with Wrist-Mounted Illuminant by Shadow Projection. In *Proceedings of the 36th Annual ACM Symposium on User Interface Software and Technology* (San Francisco, CA, USA) *(UIST '23)*. Association for Computing Machinery, New York, NY, USA, Article 27, 14 pages. doi:10.1145/3586183.3606785

[25] Yu Lu, Dian Ding, Hao Pan, Yijie Li, Juntao Zhou, Yongjian Fu, Yongzhao Zhang, Yi-Chao Chen, and Guangtao Xue. 2024. HandPad: Make Your Hand an On-the-go Writing Pad via Human Capacitance. In *Proceedings of the 37th Annual ACM Symposium on User Interface Software and Technology* (Pittsburgh, PA, USA) *(UIST '24)*. Association for Computing Machinery, New York, NY, USA, Article 4, 16 pages. doi:10.1145/3654777.3676328

[26] I Scott MacKenzie. 1992. Fitts' law as a research and design tool in human-computer interaction. *Human-computer interaction* 7, 1 (1992), 91–139.

[27] I Scott MacKenzie, Tatu Kauppinen, and Miika Silfverberg. 2001. Accuracy measures for evaluating computer pointing devices. In *Proceedings of the SIGCHI conference on Human factors in computing systems*. 9–16.

[28] Akhmajon Makhsadov, Donald Degraen, André Zenner, Felix Kosmalla, Kamila Mushkina, and Antonio Krüger. 2022. VRySmart: a Framework for Embedding Smart Devices in Virtual Reality. In *Extended Abstracts of the 2022 CHI Conference on Human Factors in Computing Systems* (New Orleans, LA, USA) *(CHI EA '22)*. Association for Computing Machinery, New York, NY, USA, Article 358, 8 pages. doi:10.1145/3491101.3519717

[29] Lawrence Makin, Gareth Barnaby, and Anne Roudaut. 2019. Tactile and kinesthetic feedbacks improve distance perception in virtual reality. In *Proceedings of the 31st Conference on l'Interaction Homme-Machine* (Grenoble, France) *(IHM '19)*. Association for Computing Machinery, New York, NY, USA, Article 2, 9 pages. doi:10.1145/3366550.3372248

[30] Manuel Meier, Paul Streli, Andreas Fender, and Christian Holz. 2021. TapID: Rapid Touch Interaction in Virtual Reality using Wearable Sensing. In *2021 IEEE Virtual Reality and 3D User Interfaces (VR)*. 519–528. doi:10.1109/VR50410.2021.00076

[31] Tzu-Wei Mi, Jia-Jun Wang, and Liwei Chan. 2023. LapTouch: Using the Lap for Seated Touch Interaction with HMDs. *Proc. ACM Interact. Mob. Wearable Ubiquitous Technol.* 7, 3, Article 114 (Sept. 2023), 23 pages. doi:10.1145/3610878

[32] Vimal Mollyn, Nathan DeVrio, and Chris Harrison. 2025. EclipseTouch: Touch Segmentation on Ad Hoc Surfaces using Worn Infrared Shadow Casting. In *Proceedings of the 38th Annual ACM Symposium on User Interface Software and Technology (UIST '25)*. Association for Computing Machinery, New York, NY, USA, Article 195, 13 pages. doi:10.1145/3746059.3747743

[33] Vimal Mollyn and Chris Harrison. 2024. EgoTouch: On-Body Touch Input Using AR/VR Headset Cameras. In *Proceedings of the 37th Annual ACM Symposium on User Interface Software and Technology* (Pittsburgh, PA, USA) *(UIST '24)*. Association for Computing Machinery, New York, NY, USA, Article 69, 11 pages. doi:10.1145/3654777.3676455

[34] Takehiro Niikura, Yoshihiro Watanabe, and Masatoshi Ishikawa. 2014. Anywhere surface touch: utilizing any surface as an input area. In *Proceedings of the 5th Augmented Human International Conference* (Kobe, Japan) *(AH '14)*. Association for Computing Machinery, New York, NY, USA, Article 39, 8 pages. doi:10.1145/2582051.2582090

[35] Manuel Prätorius, Dimitar Valkov, Ulrich Burgbacher, and Klaus Hinrichs. 2014. DigiTap: an eyes-free VR/AR symbolic input device. In *Proceedings of the 20th ACM Symposium on Virtual Reality Software and Technology* (Edinburgh, Scotland) *(VRST '14)*. Association for Computing Machinery, New York, NY, USA, 9–18. doi:10.1145/2671015.2671029

[36] Mark Richardson, Fadi Botros, Yangyang Shi, Pinhao Guo, Bradford J Snow, Linguang Zhang, Jingming Dong, Keith Vertanen, Shugao Ma, and Robert Wang. 2024. StegoType: Surface Typing from Egocentric Cameras. In *Proceedings of the 37th Annual ACM Symposium on User Interface Software and Technology* (Pittsburgh, PA, USA) *(UIST '24)*. Association for Computing Machinery, New York, NY, USA, Article 83, 14 pages. doi:10.1145/3654777.3676343

[37] Mark Richardson, Matt Durasoff, and Robert Wang. 2020. Decoding Surface Touch Typing from Hand-Tracking. In *Proceedings of the 33rd Annual ACM Symposium on User Interface Software and Technology* (Virtual Event, USA) *(UIST '20)*. Association for Computing Machinery, New York, NY, USA, 686–696. doi:10.1145/3379337.3415816

[38] Anne Roudaut, Henning Pohl, and Patrick Baudisch. 2011. Touch input on curved surfaces. In *Proceedings of the SIGCHI Conference on Human Factors in Computing Systems* (Vancouver, BC, Canada) *(CHI '11)*. Association for Computing Machinery, New York, NY, USA, 1011–1020. doi:10.1145/1978942.1979094

[39] Carolin Stellmacher, Florian Mathis, Yannick Weiss, Meagan B. Loerakker, Nadine Wagener, and Johannes Schöning. 2024. Exploring Mobile Devices as Haptic Interfaces for Mixed Reality. In *Proceedings of the 2024 CHI Conference on Human Factors in Computing Systems* (Honolulu, HI, USA) *(CHI '24)*. Association for Computing Machinery, New York, NY, USA, Article 422, 17 pages. doi:10.1145/3613904.3642176

[40] Paul Streli, Jiaxi Jiang, Andreas Rene Fender, Manuel Meier, Hugo Romat, and Christian Holz. 2022. TapType: Ten-finger text entry on everyday surfaces via Bayesian inference. In *Proceedings of the 2022 CHI Conference on Human Factors in Computing Systems* (New Orleans, LA, USA) *(CHI '22)*. Association for Computing Machinery, New York, NY, USA, Article 497, 16 pages. doi:10.1145/3491102.3501878

[41] Hemant Bhaskar Surale, Aakar Gupta, Mark Hancock, and Daniel Vogel. 2019. TabletInVR: Exploring the Design Space for Using a Multi-Touch Tablet in Virtual Reality. In *Proceedings of the 2019 CHI Conference on Human Factors in Computing Systems* (Glasgow, Scotland Uk) *(CHI '19)*. Association for Computing Machinery, New York, NY, USA, 1–13. doi:10.1145/3290605.3300243

[42] Radu-Daniel Vatavu and Bogdan-Florin Gheran. 2025. Intermanual Deictics: Uncovering Users' Gesture Preferences for Opposite-Arm Referential Input, from Fingers to Shoulder. In *Proceedings of the 2025 CHI Conference on Human Factors in Computing Systems (CHI '25)*. Association for Computing Machinery, New York, NY, USA, Article 283, 16 pages. doi:10.1145/3706598.3713474

[43] Santiago Villarreal-Narvaez, Thibaut Septon, and Bruno Dumas. 2025. Designing Touch-Based Gestures for Thigh-Worn Wearable Device in Passenger-Focused Vehicular XR Environments. In *Companion Proceedings of the 17th ACM SIGCHI Symposium on Engineering Interactive Computing Systems (EICS '25 Companion)*. Association for Computing Machinery, New York, NY, USA, 33–41. doi:10.1145/3731406.3734977

[44] Simon Voelker, Christine Sutter, Lei Wang, and Jan Borchers. 2012. Understanding flicking on curved surfaces. In *Proceedings of the SIGCHI Conference on Human Factors in Computing Systems* (Austin, Texas, USA) *(CHI '12)*. Association for Computing Machinery, New York, NY, USA, 189–198. doi:10.1145/2207676.2207703

[45] Cheng-Yao Wang, Wei-Chen Chu, Po-Tsung Chiu, Min-Chieh Hsiu, Yih-Harn Chiang, and Mike Y. Chen. 2015. PalmType: Using Palms as Keyboards for Smart Glasses. In *Proceedings of the 17th International Conference on Human-Computer Interaction with Mobile Devices and Services* (Copenhagen, Denmark) *(MobileHCI '15)*. Association for Computing Machinery, New York, NY, USA, 153–160. doi:10.1145/2785830.2785886

[46] Cheng-Yao Wang, Min-Chieh Hsiu, Po-Tsung Chiu, Chiao-Hui Chang, Liwei Chan, Bing-Yu Chen, and Mike Y. Chen. 2015. PalmGesture: Using Palms as Gesture Interfaces for Eyes-free Input. In *Proceedings of the 17th International Conference on Human-Computer Interaction with Mobile Devices and Services* (Copenhagen, Denmark) *(MobileHCI '15)*. Association for Computing Machinery, New York, NY, USA, 217–226. doi:10.1145/2785830.2785885

[47] Martin Weigel, Aditya Shekhar Nittala, Alex Olwal, and Jürgen Steimle. 2017. SkinMarks: Enabling Interactions on Body Landmarks Using Conformal Skin Electronics. In *Proceedings of the 2017 CHI Conference on Human Factors in Computing Systems* (Denver, Colorado, USA) *(CHI '17)*. Association for Computing Machinery, New York, NY, USA, 3095–3105. doi:10.1145/3025453.3025704

[48] Malte Weiss, Simon Voelker, Christine Sutter, and Jan Borchers. 2010. BendDesk: dragging across the curve. In *ACM International Conference on Interactive Tabletops and Surfaces* (Saarbrücken, Germany) *(ITS '10)*. Association for Computing Machinery, New York, NY, USA, 1–10. doi:10.1145/1936652.1936654

[49] Jacob O. Wobbrock, Leah Findlater, Darren Gergle, and James J. Higgins. 2011. The aligned rank transform for nonparametric factorial analyses using only anova procedures. In *Proceedings of the SIGCHI Conference on Human Factors in Computing Systems* (Vancouver, BC, Canada) *(CHI '11)*. Association for Computing Machinery, New York, NY, USA, 143–146. doi:10.1145/1978942.1978963

[50] Ziyi Xia, Xincheng Huang, Sidney S Fels, and Robert Xiao. 2025. HaloTouch: Using IR Multi-Path Interference to Support Touch Interactions with General Surfaces. In *Proceedings of the 2025 CHI Conference on Human Factors in Computing Systems (CHI '25)*. Association for Computing Machinery, New York, NY, USA, Article 548, 17 pages. doi:10.1145/3706598.3714179

[51] Chenhan Xu, Bing Zhou, Gurunandan Krishnan, and Shree Nayar. 2023. AO-Finger: Hands-free Fine-grained Finger Gesture Recognition via Acoustic-Optic Sensor Fusing. In *Proceedings of the 2023 CHI Conference on Human Factors in Computing Systems* (Hamburg, Germany) *(CHI '23)*. Association for Computing Machinery, New York, NY, USA, Article 306, 14 pages. doi:10.1145/3544548.3581264

[52] Sang Ho Yoon, Ke Huo, Vinh P Nguyen, and Karthik Ramani. 2015. TIMMi: Finger-worn textile input device with multimodal sensing in mobile interaction. In *Proceedings of the Ninth International Conference on Tangible, Embedded, and Embodied Interaction*. 269–272.

[53] Mingrui Ray Zhang, Shumin Zhai, and Jacob O. Wobbrock. 2022. TypeAnywhere: A QWERTY-Based Text Entry Solution for Ubiquitous Computing. In *Proceedings of the 2022 CHI Conference on Human Factors in Computing Systems* (New Orleans, LA, USA) *(CHI '22)*. Association for Computing Machinery, New York, NY, USA, Article 339, 16 pages. doi:10.1145/3491102.3517686

[54] Yang Zhang, Wolf Kienzle, Yanjun Ma, Shiu S. Ng, Hrvoje Benko, and Chris Harrison. 2019. ActiTouch: Robust Touch Detection for On-Skin AR/VR Interfaces. In *Proceedings of the 32nd Annual ACM Symposium on User Interface Software and Technology* (New Orleans, LA, USA) *(UIST '19)*. Association for Computing Machinery, New York, NY, USA, 1151–1159. doi:10.1145/3332165.3347869

[55] Graeme Zinck, Roya Cody, Che Yan, Da-Yuan Huang, Wei Li, and Daniel Vogel. 2023. Evaluating Across-Hinge Dragging with Pen and Touch on Curved and Foldable Displays. In *Proceedings of the 2023 CHI Conference on Human Factors in Computing Systems* (Hamburg, Germany) *(CHI '23)*. Association for Computing Machinery, New York, NY, USA, Article 314, 12 pages. doi:10.1145/3544548.3580825